

Supporting Information

Re-parameterization of RNA χ torsion parameters for the AMBER force field and comparison to NMR spectra for cytidine and uridine

Ilyas Yildirim, Harry A. Stern, Scott D. Kennedy, Jason D. Tubbs and Douglas H. Turner

Department of Chemistry and Center for RNA Biology, University of Rochester, Rochester, New York 14627, and

Department of Biochemistry and Biophysics, School of Medicine and Dentistry, University of Rochester,

Rochester, New York 14642

yildirim@pas.rochester.edu,

hstern@chem.rochester.edu,

scott_kennedy@urmc.rochester.edu,

jason.tubbs@rochester.edu, turner@chem.rochester.edu

- Table S1.** Frozen dihedrals during QM optimization in PES scan.
- Table S2.** Restrained dihedral angles in the MM minimization to calculate the MM energies, $E_{MM}^{(noCHI)}$.
- Table S3.** Sample restraint file.
- Table S4.** Temperature vs. chemical shift of different protons of U and C for sample concentrations of 0.2, 1.0, and 5.0 mM.
- Table S5.** Temperature vs. chemical shift of different protons of A and G for sample concentrations of 0.2, 1.0, and 5.0 mM.
- Table S6.** Sugar pucker conformations used to test the AMBER99, AMBER99 χ , and Ode force fields.
- Table S7.** NOE data from transient NOE experiments and anti/syn proportions of C and U.
- Table S8.** Population analysis results for C, U, A, and G.
- Table S9.** Predicted ΔG° (in kcal/mol) values of C2'→C3' and syn→anti transformations.
- Table S10.** Percentage NOE data extracted from SSNOE experiments for C and U.
- Table S11.** 3J spin-spin couplings and experimentally deduced sugar puckering of 5 mM C, and 5 mM U.
- Table S12.** 3J spin-spin couplings and experimentally deduced sugar puckering of 0.2 mM A, and 0.2 mM G.
- Table S13.** Experimentally deduced and force field predicted base orientation around glycosidic dihedral angle and sugar puckering for C, U, A, and G, and ΔG° of C2'→C3' and syn→anti transformations for C, and U.
- Table S14.** % of anti conformation for each individual 30 ns simulation.
- Table S15.** % of anti conformation of individual simulations of cytidine with AMBER99 χ force field for simulation times of 30, 60, and 120 ns.
- Figure S1.** Testing how well AMBER99, AMBER99 χ , and Ode force fields mimic the quantum mechanical energy surface of adenosine when sugar pucker is C2'endo.
- Figure S2.** Testing how well AMBER99, AMBER99 χ , and Ode force fields mimic the quantum mechanical energy surface of adenosine when sugar pucker is C3'endo.
- Figure S3.** Testing how well AMBER99, AMBER99 χ , and Ode force fields mimic the quantum mechanical energy surface of adenosine when sugar pucker is O4'endo.
- Figure S4.** Testing how well AMBER99, AMBER99 χ , and Ode force fields mimic the quantum mechanical energy surface of guanosine when sugar pucker is C2'endo.

- Figure S5.** Testing how well AMBER99, AMBER99 χ , and Ode force fields mimic the quantum mechanical energy surface of guanosine when sugar pucker is C3'endo.
- Figure S6.** Testing how well AMBER99, AMBER99 χ , and Ode force fields mimic the quantum mechanical energy surface of guanosine when sugar pucker is O4'endo.
- Figure S7.** Testing how well AMBER99, AMBER99 χ , and Ode force fields mimic the quantum mechanical energy surface of cytidine when sugar pucker is C2'endo.
- Figure S8.** Testing how well AMBER99, AMBER99 χ , and Ode force fields mimic the quantum mechanical energy surface of cytidine when sugar pucker is C3'endo.
- Figure S9.** Testing how well AMBER99, AMBER99 χ , and Ode force fields mimic the quantum mechanical energy surface of cytidine when sugar pucker is O4'endo.
- Figure S10.** Testing how well AMBER99, AMBER99 χ , and Ode force fields mimic the quantum mechanical energy surface of uridine when sugar pucker is C2'endo.
- Figure S11.** Testing how well AMBER99, AMBER99 χ , and Ode force fields mimic the quantum mechanical energy surface of uridine when sugar pucker is C3'endo.
- Figure S12.** Testing how well AMBER99, AMBER99 χ , and Ode force fields mimic the quantum mechanical energy surface of uridine when sugar pucker is O4'endo.
- Figure S13.** Intensity vs. mixing time plot of H5, H2', and H1' protons in transient NOE NMR experiment for 5 mM sample of cytidine at 10°C.
- Figure S14.** Intensity vs. mixing time plot of H5, H2', and H1' protons in transient NOE NMR experiment for 5 mM sample of uridine at 10°C.
- Figure S15.** RMSD vs. time plots of MD simulations of adenosine and guanosine.
- Figure S16.** RMSD vs. time plots of MD simulations of cytidine and uridine.
- Figure S17.** Population distributions of χ torsion angles of cytidine and uridine for convergence analysis.
- Figure S18.** Population distributions of χ torsion angles of adenosine and guanosine for convergence analysis.

Table S1. Frozen dihedrals during QM optimization in PES scan.^a

| Dihedral | Cytidine | Uridine | Adenosine | Guanosine |
|------------------|------------------|------------------|------------------|------------------|
| H5T-O5'-C5'-C4' | (60,174) | (60,174) | (60,174) | (60,174) |
| O5'-C5'-C4'-C3' | 54 | 54 | 54 | 54 |
| C5'-C4'-C3'-O3' | (140,81) | (140,81) | (140,81) | (140,81) |
| C4'-C3'-O3'-H3T | -148 | -148 | -148 | -148 |
| O4'-C1'-C2'-C3' | (32,-24) | (32,-24) | (32,-24) | (32,-24) |
| C1'-C2'-O2'-HO'2 | (-61,21,-153,93) | (-61,21,-153,93) | (-61,21,-153,93) | (-61,21,-153,93) |
| C1'-C8-N9-C4 | - | - | 180 | 180 |
| N9-N3-C4-C5 | - | - | 180 | 180 |
| C6-H61-N6-H62 | - | - | 180 | - |
| C2-H21-N2-H22 | - | - | - | 180 |
| C1'-C6-N1-C2 | 180 | 180 | - | - |
| C4-H41-N4-H42 | 180 | - | - | - |
| C4-C5-N7-C8 | - | - | 0.0 | 0.0 |
| C4-C5-C6-N1 | - | - | 0.0 | 0.0 |
| C6-N1-C2-N3 | - | - | 0.0 | 0.0 |
| N1-C2-N3-C4 | 0.0 | 0.0 | - | - |
| N3-C4-C5-C6 | 0.0 | 0.0 | - | - |

^a The values in parenthesis mean the sugar conformations used in the PES scan defined in Table 1.

Table S2. Restrained dihedral angles in the MM minimization to calculate the MM energies, $E_{MM}^{(noCHI)}$. X denotes the dihedral restraints that are used for that torsion angle.

| Dihedral | Cytidine | Uridine | Adenosine | Guanosine |
|------------------|----------|---------|-----------|-----------|
| H5T-O5'-C5'-C4' | X | X | X | X |
| O5'-C5'-C4'-C3' | X | X | X | X |
| C5'-C4'-C3'-O3' | X | X | X | X |
| C4'-C3'-O3'-H3T | X | X | X | X |
| O4'-C1'-C2'-C3' | X | X | X | X |
| C1'-C2'-O2'-HO'2 | X | X | X | X |
| O4'-C1'-N9-C8 | - | - | X | X |
| C2'-C1'-N9-C8 | - | - | X | X |
| O4'-C1'-N1-C6 | X | X | - | - |
| C2'-C1'-N1-C2 | X | X | - | - |
| C1'-C8-N9-C4 | - | - | X | X |
| N9-N3-C4-C5 | - | - | X | X |
| C6-H61-N6-H62 | - | - | X | - |
| C2-H21-N2-H22 | - | - | - | X |
| C1'-C6-N1-C2 | X | X | - | - |
| C4-H41-N4-H42 | X | - | - | - |
| C4-C5-N7-C8 | - | - | X | X |
| C4-C5-C6-N1 | - | - | X | X |
| C6-N1-C2-N3 | - | - | X | X |
| N1-C2-N3-C4 | X | X | - | - |
| N3-C4-C5-C6 | X | X | - | - |

Table S3. Sample restraint file, RST, used in the minimization procedure of adenosine.^a

```
# 1 RAN Beta: (1 RAN H5T)-(1 RAN O5')-(1 RAN C5')-(1 RAN C4') 60.04
&rst iat = 1,2,3,6,
      r1 = 58.03, r2 = 60.03, r3 = 60.05, r4 = 62.05,
      rk2 = 1500.0, rk3 = 1500.0, ialtd=0, &end
# 1 RAN Gamma: (1 RAN O5')-(1 RAN C5')-(1 RAN C4')-(1 RAN C3') 53.99
&rst iat = 2,3,6,25,
      r1 = 51.98, r2 = 53.98, r3 = 54, r4 = 56, &end
# 1 RAN Delta: (1 RAN C5')-(1 RAN C4')-(1 RAN C3')-(1 RAN O3') 140.01
&rst iat = 3,6,25,31,
      r1 = 138, r2 = 140, r3 = 140.02, r4 = 142.02, &end
# 1 RAN Epsilon: (1 RAN C4')-(1 RAN C3')-(1 RAN O3')-(1 RAN H3T) 212.01
&rst iat = 6,25,31,32,
      r1 = 210, r2 = 212, r3 = 212.02, r4 = 214.02, &end
# 1 RAN SUGAR1 (C3'endo): (1 RAN O4')-(1 RAN C1')-(1 RAN C2')-(1 RAN C3') 32.04
&rst iat = 8,9,27,25,
      r1 = 30.03, r2 = 32.03, r3 = 32.05, r4 = 34.05, &end
# 1 RAN SUGAR2 (2'-OH group): (1 RAN C1')-(1 RAN C2')-(1 RAN O2')-(1 RAN HO'2)
# 298.99
&rst iat = 9,27,29,30,
      r1 = 296.98, r2 = 298.98, r3 = 299, r4 = 301, &end
# 1 RAN CHI1: (1 RAN O4')-(1 RAN C1')-(1 RAN N9)-(1 RAN C8) 0.02
&rst iat = 8,9,11,12,
      r1 = -1.99, r2 = 0.01, r3 = 0.03, r4 = 2.03, &end
# 1 RAN CHI2: (1 RAN C2')-(1 RAN C1')-(1 RAN N9)-(1 RAN C8) 244.25
&rst iat = 27,9,11,12,
      r1 = 242.24, r2 = 244.24, r3 = 244.26, r4 = 246.26, &end
# 1 RAN IMP1: (1 RAN C1')-(1 RAN C8)-(1 RAN N9)-(1 RAN C4) 180.04
&rst iat = 9,12,11,24,
      r1 = 178.03, r2 = 180.03, r3 = 180.05, r4 = 182.05, &end
# 1 RAN IMP2: (1 RAN N9)-(1 RAN N3)-(1 RAN C4)-(1 RAN C5) 180.00
&rst iat = 11,23,24,15,
      r1 = 177.99, r2 = 179.99, r3 = 180.01, r4 = 182.01, &end
# 1 RAN IMP3: (1 RAN C6)-(1 RAN H61)-(1 RAN N6)-(1 RAN H62) 179.97
&rst iat = 16,18,17,19,
      r1 = 177.96, r2 = 179.96, r3 = 179.98, r4 = 181.98, &end
# 1 RAN PRP1: (1 RAN C4)-(1 RAN C5)-(1 RAN N7)-(1 RAN C8) 359.99
&rst iat = 24,15,14,12,
      r1 = 357.98, r2 = 359.98, r3 = 360, r4 = 362, &end
# 1 RAN PRP2: (1 RAN C4)-(1 RAN C5)-(1 RAN C6)-(1 RAN N1) 0.00
&rst iat = 24,15,16,20,
      r1 = -2.01, r2 = -0.01, r3 = 0.01, r4 = 2.01, &end
# 1 RAN PRP3: (1 RAN C6)-(1 RAN N1)-(1 RAN C2)-(1 RAN N3) 359.97
&rst iat = 16,20,21,23,
      r1 = 357.96, r2 = 359.96, r3 = 359.98, r4 = 361.98, &end
```

^a This restraint file is used in the sander module of AMBER9 to restrain the dihedral angles of the structures to the QM optimized structures in the minimization protocol. It is also called NMR restraint file, which is the only method that can be used by sander to restrain the dihedral angles.

Table S4. Temperature (in °C) vs. chemical shift (ppm) of different protons of U and C for nucleoside concentrations of 0.2, 1.0, and 5.0 mM.

| Uridine | | | | | Cytidine | | | | |
|---------|-------|-------|-------|-------|----------|-------|-------|-------|-------|
| 0.2 mM | | | | | 0.2 mM | | | | |
| TEMP | H6 | H5 | H1' | H2' | TEMP | H6 | H5 | H1' | H2' |
| 0 | 7.919 | 5.888 | 5.929 | 4.358 | 0 | 7.878 | 6.051 | 5.912 | 4.315 |
| 10 | 7.912 | 5.907 | 5.937 | 4.369 | 10 | 7.874 | 6.065 | 5.921 | 4.323 |
| 20 | 7.895 | 5.912 | 5.933 | 4.369 | 20 | 7.860 | 6.069 | 5.919 | 4.323 |
| 30 | 7.878 | 5.915 | 5.928 | 4.368 | 30 | 7.849 | 6.072 | 5.917 | 4.323 |
| 40 | 7.863 | 5.918 | 5.922 | 4.368 | 40 | 7.837 | 6.074 | 5.915 | 4.322 |
| 50 | 7.850 | - | - | 4.371 | 50 | 7.829 | 6.079 | - | 4.324 |
| 60 | 7.841 | - | - | - | 60 | 7.825 | 6.088 | - | - |
| 1.0 mM | | | | | 1 mM | | | | |
| TEMP | H6 | H5 | H1' | H2' | TEMP | H6 | H5 | H1' | H2' |
| 0 | 7.920 | 5.889 | 5.929 | 4.358 | 0 | 7.877 | 6.050 | 5.912 | 4.313 |
| 10 | 7.912 | 5.906 | 5.936 | 4.369 | 10 | 7.873 | 6.064 | 5.920 | 4.322 |
| 20 | 7.895 | 5.912 | 5.933 | 4.369 | 20 | 7.860 | 6.068 | 5.919 | 4.323 |
| 30 | 7.879 | 5.916 | 5.929 | 4.369 | 30 | 7.848 | 6.072 | 5.917 | 4.323 |
| 40 | 7.863 | - | - | 4.369 | 40 | 7.836 | 6.072 | 5.913 | 4.322 |
| 50 | 7.850 | - | - | 4.371 | 50 | 7.828 | 6.077 | 5.913 | 4.324 |
| 60 | 7.841 | - | - | - | 60 | 7.824 | 6.082 | 5.915 | - |
| 5.0 mM | | | | | 5 mM | | | | |
| TEMP | H6 | H5 | H1' | H2' | TEMP | H6 | H5 | H1' | H2' |
| 0 | 7.921 | 5.889 | 5.929 | 4.358 | 0 | 7.878 | 6.050 | 5.913 | 4.313 |
| 10 | 7.913 | 5.907 | 5.937 | 4.369 | 10 | 7.874 | 6.064 | 5.922 | 4.325 |
| 20 | 7.895 | 5.910 | 5.933 | 4.369 | 20 | 7.861 | 6.069 | 5.920 | 4.323 |
| 30 | 7.879 | 5.916 | 5.929 | 4.370 | 30 | 7.848 | 6.072 | 5.917 | 4.324 |
| 40 | 7.863 | 5.918 | 5.922 | 4.369 | 40 | 7.836 | 6.073 | 5.914 | 4.323 |
| 50 | 7.851 | - | - | 4.372 | 50 | 7.828 | 6.074 | 5.913 | 4.324 |
| 60 | 7.841 | - | - | 4.377 | 60 | 7.824 | 6.082 | 5.915 | 4.330 |

Table S5. Temperature (in °C) vs. chemical shift (ppm) of different protons of A and G for different nucleoside concentrations. Guanosine at 5 mM could not be analyzed due to association.

| Adenosine | | | | | Guanosine | | | | |
|-----------|-------|-------|-------|-------|-----------|-------|-------|-------|-------|
| 0.2 mM | | | | | 0.2 mM | | | | |
| TEMP | H8 | H2 | H1' | H2' | TEMP | H8 | H1' | H2' | H3' |
| 0 | 8.348 | 8.248 | 6.080 | 4.825 | 2 | 7.967 | 5.874 | 4.702 | 4.367 |
| 10 | 8.359 | 8.267 | 6.093 | 4.830 | 10 | 7.977 | 5.885 | 4.710 | 4.378 |
| 20 | 8.358 | 8.274 | 6.092 | - | 20 | 7.982 | 5.893 | - | 4.386 |
| 30 | 8.356 | 8.280 | 6.092 | - | 30 | 7.980 | 5.895 | - | 4.389 |
| 40 | 8.351 | 8.284 | 6.091 | 4.813 | 40 | 7.973 | 5.891 | - | 4.386 |
| 50 | 8.349 | 8.290 | 6.093 | 4.810 | 50 | 7.961 | 5.885 | 4.699 | 4.376 |
| 60 | 8.350 | 8.300 | 6.098 | 4.812 | 60 | 7.946 | 5.874 | 4.688 | - |
| 1 mM | | | | | 1 mM | | | | |
| TEMP | H8 | H2 | H1' | H2' | TEMP | H8 | H1' | H2' | H3' |
| 0 | 8.345 | 8.240 | 6.078 | 4.822 | 2 | 7.966 | 5.873 | 4.702 | 4.366 |
| 10 | 8.356 | 8.261 | 6.090 | 4.828 | 10 | 7.975 | 5.884 | 4.710 | 4.378 |
| 20 | 8.355 | 8.270 | 6.091 | - | 20 | 7.980 | 5.891 | 4.714 | 4.384 |
| 30 | 8.354 | 8.277 | 6.092 | - | 30 | 7.979 | 5.894 | - | 4.389 |
| 40 | 8.350 | 8.282 | 6.091 | 4.812 | 40 | 7.972 | 5.892 | 4.710 | 4.387 |
| 50 | 8.351 | 8.291 | 6.094 | 4.812 | 50 | 7.961 | 5.886 | 4.702 | 4.382 |
| 60 | 8.350 | 8.302 | 6.098 | 4.811 | 60 | 7.945 | 5.876 | 4.691 | - |
| 5 mM | | | | | | | | | |
| TEMP | H8 | H2 | H1' | H2' | | | | | |
| 0 | 8.323 | 8.191 | 6.059 | 4.806 | | | | | |
| 10 | 8.341 | 8.228 | 6.077 | 4.817 | | | | | |
| 20 | 8.345 | 8.246 | 6.082 | - | | | | | |
| 30 | 8.345 | 8.260 | 6.084 | - | | | | | |
| 40 | 8.344 | 8.270 | 6.085 | 4.808 | | | | | |
| 50 | 8.345 | 8.280 | 6.089 | 4.807 | | | | | |
| 60 | 8.346 | 8.292 | 6.095 | 4.809 | | | | | |

Table S6. Sugar pucker conformations used to test how well AMBER99, AMBER99 χ , and Ode force fields mimic the quantum mechanical energy surfaces shown in Figures S1-S12.

| Dihedral | C2'endo | C3'endo | O4'endo |
|------------------|----------------|----------------|----------------|
| H5T-O5'-C5'-C4' | (174,60) | (174,60) | (174,60) |
| O5'-C5'-C4'-C3' | 54 | 54 | 54 |
| C5'-C4'-C3'-O3' | 140 | 81 | 81 |
| C4'-C3'-O3'-H3T | -148 | -148 | -148 |
| O4'-C1'-C2'-C3' | 32 | -24 | 32 |
| C1'-C2'-O2'-HO'2 | (-61,21) | (-153,93) | (-61,21) |

Table S7. NOE data from transient NOE experiments and anti/syn proportions deduced using two-state model for 5 mM C and 5 mM U upon irradiation of H6 proton.

| Nucleoside (and Temperature in °C) | Mixing time (s) | NOE (%) H5 | NOE (%) H1' | anti ^a (%) |
|---------------------------------------|--------------------|---------------|----------------|--------------------------|
| Cytidine (2 °C) | 0.2 | 1.198 | 0.581 | 85 |
| | 0.3 | 1.680 | 0.790 | 86 |
| | 0.4 | 2.046 | 0.973 | 82 |
| Average | | | | 84 |
| Cytidine (10 °C) | 0.2 | 1.183 | 0.521 | 87 |
| | 0.3 | 1.798 | 0.776 | 88 |
| | 0.4 | 2.209 | 1.068 | 86 |
| Average | | | | 87 |
| Uridine (10 °C) | 0.2 | 1.504 | 0.388 | 95 |
| | 0.3 | 1.963 | 0.626 | 92 |
| | 0.4 | 2.376 | 0.837 | 91 |
| Average | | | | 93 |

^a Two-state model where the nucleosides were assumed to have either syn or anti conformations was used to calculate the proportion of anti conformations. H5 NOE, which is used as reference NOE, corresponds to a distance of 2.48 Å. In anti and syn conformations, H1'-H6 distance is 3.48 Å and 2.12 Å, respectively. These values correspond to the minimum energies in the PES scan of pyrimidines. See text for details.

Table S8. Population analysis results for C, U, A, and G of the AMBER99 and AMBER99 χ force fields (see Figures 6 and 7 in text for conformations corresponding to i-vi).

| | (i) (%) | (ii) (%) | (iii) (%) | (iv) (%) | (v) (%) | (vi) (%) | C2'endo ^a (%) | C3'endo ^b (%) | anti ^c (%) | syn ^d (%) |
|---------------------------------|------------|-------------|--------------|-------------|------------|-------------|-----------------------------|-----------------------------|--------------------------|-------------------------|
| AMBER99 | | | | | | | | | | |
| Cytidine | 52 | 16 | 19 | 11 | - | - | 71 | 27 | 30 | 68 |
| Uridine | 47 | 24 | 17 | 11 | - | - | 64 | 35 | 28 | 71 |
| Adenosine | 57 | 21 | - | - | 12 | 3 | 69 | 24 | 15 ^e | 78 |
| Guanosine | 54 | 31 | - | - | 7 | 4 | 61 | 35 | 11 ^e | 85 |
| AMBER99χ | | | | | | | | | | |
| Cytidine | 20 | 10 | 25 | 44 | - | - | 45 | 54 | 69 | 30 |
| Uridine | 9 | 8 | 36 | 47 | - | - | 44 | 55 | 83 | 17 |
| Adenosine | 59 | 24 | 5 | 8 | - | - | 64 | 32 | 13 | 83 |
| Guanosine | 33 | 39 | 9 | 15 | 2 | - | 44 | 54 | 26 | 72 |

^a % C2'endo = (i)+(iii)+(v), ^b % C3'endo = (ii)+(iv)+(vi), ^c % anti = (iii)+(iv), ^d % syn = (i)+(ii), ^e These values represent population of high-anti conformations.

Table S9. Predicted ΔG° (in kcal/mol) values of C2'→C3' and syn→anti transformations of the experimental and computational methods for C and U.^a

| | NMR | | AMBER99 | | AMBER99 χ | |
|----------|---|--|--|---|--|---|
| | $\Delta G^\circ_{C2' \rightarrow C3'}$ ^b | $\Delta G^\circ_{syn \rightarrow anti}$ ^c | $\Delta G^\circ_{C2' \rightarrow C3'}$ | $\Delta G^\circ_{syn \rightarrow anti}$ | $\Delta G^\circ_{C2' \rightarrow C3'}$ | $\Delta G^\circ_{syn \rightarrow anti}$ |
| Cytidine | -0.24 | -1.07 | 0.58 | 0.49 | -0.11 | -0.50 |
| Uridine | -0.15 | -1.45 | 0.36 | 0.55 | -0.13 | -0.95 |

^a For a transformation of A→B, $\Delta G^\circ_{A \rightarrow B} = -RT \ln(K)$, where $R=1.987 \text{ cal K}^{-1} \text{ mol}^{-1}$, T is the temperature in Kelvin, and K is the ratio of concentrations of each species, [B]/[A]. Tables S7 and S8 were used to calculate the equilibration constant K. ^b These values are for 30°C (Table 4 in the text). ^c These values are extracted from transient NOE experiments at 10°C, while the simulations are done at 300 K (Table S7).

Table S10. Percentage NOE data extracted from SSNOE experiments for 5 mM C and 5 mM U upon irradiation of H6 proton.

| Nucleoside | Temperature (°C) | NOE (%) H1' | NOE (%) H2'+H3' | χ type |
|------------|------------------|----------------|-----------------------------|-------------|
| Cytidine | 2 | 5.9 | 9.3 (6.7+2.6) ^a | anti |
| Cytidine | 10 | 7.2 | 10.6 (7.8+2.8) ^a | anti |
| Uridine | 10 | 7.5 | 11.1 (8.6+2.5) ^a | anti |

^a Values in parenthesis represent individual percentage NOEs of H2' and H3', respectively. If the sum of % NOE from H6 to H2' and H3' is greater than the % NOE from H6 to H1', then the nucleoside prefers anti conformation.¹

Table S11. 3J spin-spin couplings (Hz) and experimentally deduced sugar puckering of 5 mM C, and 5 mM U. The subscripts of 1', 2', 3', 4', 5 and 6 in the 3J notation represent the H1', H2', H3', H4', H5, and H6 protons, respectively.

| Nucleoside | Temperature (°C) | $^3J_{1'2'}$ | $^3J_{2'3'}$ | $^3J_{3'4'}$ | $^3J_{56}$ | % C3'-endo ^a |
|------------|------------------|--------------|--------------|--------------|------------|-------------------------|
| Cytidine | 0 | 3.80 | 5.35 | 6.33 | 7.60 | 62 |
| | 5 | 3.91 | 5.24 | 6.34 | 7.55 | 62 |
| | 10 | 4.00 | 5.39 | 6.41 | 7.62 | 62 |
| | 15 | 3.99 | 5.31 | 6.27 | 7.52 | 61 |
| | 20 | 4.00 | 5.41 | 6.17 | 7.58 | 61 |
| | 25 | 4.00 | 5.49 | 6.26 | 7.60 | 61 |
| | 30 | 4.02 | 5.49 | 6.15 | 7.55 | 60 |
| | 35 | 4.07 | 5.51 | 6.16 | 7.43 | 60 |
| | 40 | 4.02 | 5.48 | 6.10 | 7.64 | 60 |
| Uridine | 0 | 4.30 | 5.45 | 6.12 | 8.16 | 59 |
| | 5 | 4.41 | 5.46 | 6.01 | 8.14 | 58 |
| | 10 | 4.43 | 5.49 | 5.98 | 8.11 | 57 |
| | 15 | 4.50 | 5.46 | 5.90 | 8.13 | 57 |
| | 20 | 4.53 | 5.45 | 5.87 | 8.17 | 56 |
| | 25 | 4.57 | 5.50 | 5.91 | 8.16 | 56 |
| | 30 | 4.59 | 5.45 | 5.77 | 8.11 | 56 |
| | 35 | 4.50 | 5.41 | 5.91 | 8.16 | 57 |
| | 40 | 4.50 | 5.52 | 5.94 | 8.11 | 57 |

^a Eq 5 is used to calculate the C3'-endo sugar pucker.

Table S12. 3J spin-spin couplings (Hz) and experimentally deduced sugar puckering of 0.2 mM A, and 0.2 mM G. The subscripts of 1', 2', 3', and 4' in the 3J notation represent the H1', H2', H3', and H4' protons, respectively.

| Nucleoside | Temperature (°C) | $^3J_{1'2'}$ | $^3J_{2'3'}$ | $^3J_{3'4'}$ | % C3'-endo ^a |
|------------|---------------------|--------------|--------------|--------------|-------------------------|
| Adenosine | 0 | 6.3 | 5.3 | 3.2 | 34 |
| | 10 | 6.2 | 5.2 | 3.2 | 34 |
| | 20 | 6.0 | 5.0 | 3.3 | 36 |
| | 30 | 6.0 | 5.1 | 3.5 | 37 |
| Guanosine | 2 | 6.3 | 5.7 | 3.5 | 36 |
| | 10 | 6.1 | 5.7 | 3.6 | 37 |
| | 20 | 6.0 | 5.5 | 3.9 | 39 |
| | 30 | 5.9 | 5.3 | 4.1 | 41 |
| | 40 | 6.0 | 5.4 | 4.9 | 45 |

^a Eq 5 is used to calculate the C3'-endo sugar pucker.

Table S13. Experimentally deduced and force field predicted base orientation around glycosidic dihedral angle and sugar puckering for C, U, A, and G, and ΔG° (in kcal/mol) of C2'→C3' and syn→anti transformations for C, and U.^a

| | | | Cytidine | Uridine | Adenosine | Guanosine |
|----------------|--|------------|----------|---------|-----------------|-----------------|
| NMR | Base Orientation ^b | % anti | 87 | 93 | - | - |
| | | % syn | 13 | 7 | - | - |
| | Sugar Puckering ^c | % C2'-endo | 40 | 44 | 63 ^d | 59 ^d |
| | | % C3'-endo | 60 | 56 | 37 ^d | 41 ^d |
| | $\Delta G^\circ_{\text{syn} \rightarrow \text{anti}}$ ^b | | -1.07 | -1.45 | - | - |
| | $\Delta G^\circ_{\text{C2}' \rightarrow \text{C3}'}$ ^c | | -0.24 | -0.15 | - | - |
| AMBER99 | Base Orientation | % anti | 30 | 28 | 15 ^e | 11 ^e |
| | | % syn | 68 | 71 | 78 | 85 |
| | Sugar Puckering | % C2'-endo | 71 | 64 | 69 | 61 |
| | | % C3'-endo | 27 | 35 | 24 | 35 |
| | $\Delta G^\circ_{\text{syn} \rightarrow \text{anti}}$ | | 0.49 | 0.55 | - | - |
| | $\Delta G^\circ_{\text{C2}' \rightarrow \text{C3}'}$ | | 0.58 | 0.36 | - | - |
| AMBER99 χ | Base Orientation | % anti | 69 | 83 | 13 ^f | 24 ^f |
| | | % syn | 30 | 17 | 83 | 72 |
| | Sugar Puckering | % C2'-endo | 45 | 44 | 64 | 44 |
| | | % C3'-endo | 54 | 55 | 32 | 54 |
| | $\Delta G^\circ_{\text{syn} \rightarrow \text{anti}}$ | | -0.50 | -0.95 | - | - |
| | $\Delta G^\circ_{\text{C2}' \rightarrow \text{C3}'}$ | | -0.11 | -0.13 | - | - |

^a For a transformation of A→B, $\Delta G^\circ_{\text{A} \rightarrow \text{B}} = -RT \ln(K)$, where $R=1.987 \text{ cal K}^{-1} \text{ mol}^{-1}$, T is the temperature in kelvin, and K is the ratio of concentrations of each species, [B]/[A] (see Table S9). ^b Predictions of the anti/syn proportions of pyrimidines are extracted from transient NOE experiments at 10 °C, while the simulations are done at 300 K (27 °C). NMR spectra on cytidine at 2 °C and 10 °C indicate essentially no temperature dependence for the anti/syn equilibrium (see Table S7). ^c These values are for 30 °C (see Tables S9 and S11). ^d These values are for 0.2 mM samples of A and G at 30 °C (see Table S12). ^e These values represent populations of high-anti conformations with $\chi \approx 310^\circ$ (see Table S8 and Figure 7 in main text). ^f These values represent populations of anti conformations with $\chi \approx 185^\circ$ (see Table S8 and Figure 7 in main text).

Table S14. % of anti conformation for each individual simulation.^a

| Start. Conf. | Sim # | Cytidine | | Uridine | | Adenosine | | Guanosine | |
|-----------------|-------|-----------|------------|-----------|------------|------------------|------------|------------------|------------|
| | | A99 | A99 χ | A99 | A99 χ | A99 ^b | A99 χ | A99 ^b | A99 χ |
| anti | 1 | 22 (7) | 73 (16) | 24 (17) | 73 (10) | 29 | 14 (17) | 33 | 35 (13) |
| | 2 | 38 (13) | 68 (16) | 18 (16) | 80 (8) | 28 | 18 (23) | 27 | 19 (17) |
| | 3 | 31 (12) | 76 (18) | 23 (17) | 86 (9) | 29 | 20 (23) | 28 | 22 (9) |
| | 4 | 28 (9) | 58 (23) | 14 (17) | 86 (9) | 24 | 10 (9) | 26 | 15 (11) |
| | 5 | 39 (15) | 63 (17) | 58 (27) | 87 (8) | 26 | 21 (13) | 29 | 38 (24) |
| Ave. | | 32 (11) | 68 (18) | 27 (19) | 82 (9) | 27 | 17 (17) | 29 | 26 (15) |
| syn | 6 | 32 (10) | 68 (17) | 31 (25) | 77 (15) | 20 | 12 (16) | 28 | 24 (12) |
| | 7 | 21 (17) | 55 (17) | 24 (18) | 86 (9) | 30 | 17 (20) | 29 | 31 (14) |
| | 8 | 53 (14) | 70 (16) | 28 (13) | 84 (9) | 27 | 22 (22) | 29 | 26 (17) |
| | 9 | 24 (9) | 56 (23) | 38 (20) | 86 (11) | 30 | 17 (16) | 25 | 36 (20) |
| | 10 | 31 (19) | 79 (12) | 30 (29) | 79 (13) | 26 | 11 (11) | 34 | 27 (15) |
| | 11 | - | 84 (17) | - | - | - | - | - | - |
| Ave. | | 32 (14) | 69 (17) | 30 (21) | 82 (11) | 27 | 16 (17) | 29 | 29 (16) |
| Total Ave. | | 31.9 (13) | 68.2 (17) | 28.8 (20) | 82.4 (10) | 26.9 | 16.2 (17) | 28.8 | 27.3 (16) |
| Sample St. Dev. | | 9.6 | 9.5 | 12.3 | 4.8 | 3.1 | 4.3 | 2.8 | 7.6 |

^a Results show % of anti conformation for each 30 ns individual simulation except for AMBER99 χ cytidine, which has 120 ns individual simulations. The latter was done to check for convergence. See Table S15 for detail. The fraction of syn population was calculated (region of $0 < \chi < 130$) and the fraction of anti population was calculated as % anti = 1 - % syn. For simulations of adenosine and guanosine with AMBER99 force field, results show a % of high-anti population. Simulations with AMBER99 force field for A and G show overlap region of high-anti and syn populations in the population distribution plot, which makes the analysis hard to interpret (see Figure S18).

Comparison to the results of Table 3 show big differences for the purines simulated with AMBER99 force field. This is due to the overlap of the high-anti and syn regions. Table 3 uses 2D population distributions to extract the fractions of anti populations (Figures 6 and 7), while the analysis presented here uses 1D population distributions (Figures S17 and S18). Errors shown are sample standard deviations. Values in parenthesis show the number of syn↔anti transformations in the simulations. ^b Numbers of transformations were not counted, but are large (see Figure S15).

Table S15. % of anti conformation of individual simulations of cytidine with AMBER99 χ force field for simulation times of 30, 60, and 120 ns. Values in parenthesis show the number of syn \leftrightarrow anti transformations in the simulations.

| | A99 χ 30 ns | A99 χ 60 ns | A99 χ 120 ns |
|------------------------------|---------------------|---------------------|----------------------|
| anti | 94 | 69 | 73 (16) |
| | 42 | 62 | 68 (16) |
| | 93 | 95 | 76 (18) |
| | 71 | 68 | 58 (23) |
| | 71 | 63 | 63 (17) |
| Average | 74 | 71 | 68 |
| syn | 81 | 75 | 68 (17) |
| | 63 | 74 | 55 (17) |
| | 51 | 53 | 70 (16) |
| | 53 | 60 | 56 (23) |
| | 89 | 88 | 79 (12) |
| | 64 | 81 | 84 (17) |
| Average | 67 | 72 | 69 |
| Total Average | 70.2 | 71.6 | 68.2 (17) |
| Sample Standard Deviation | 17.6 | 12.6 | 9.5 |

Figure S1. Testing how well AMBER99, AMBER99 χ , and Ode force fields mimic the quantum mechanical energy surface of adenosine when sugar pucker is C2'endo. Conformations used are defined in Table S6. [parm99=AMBER99; parmCHI = AMBER99 χ]

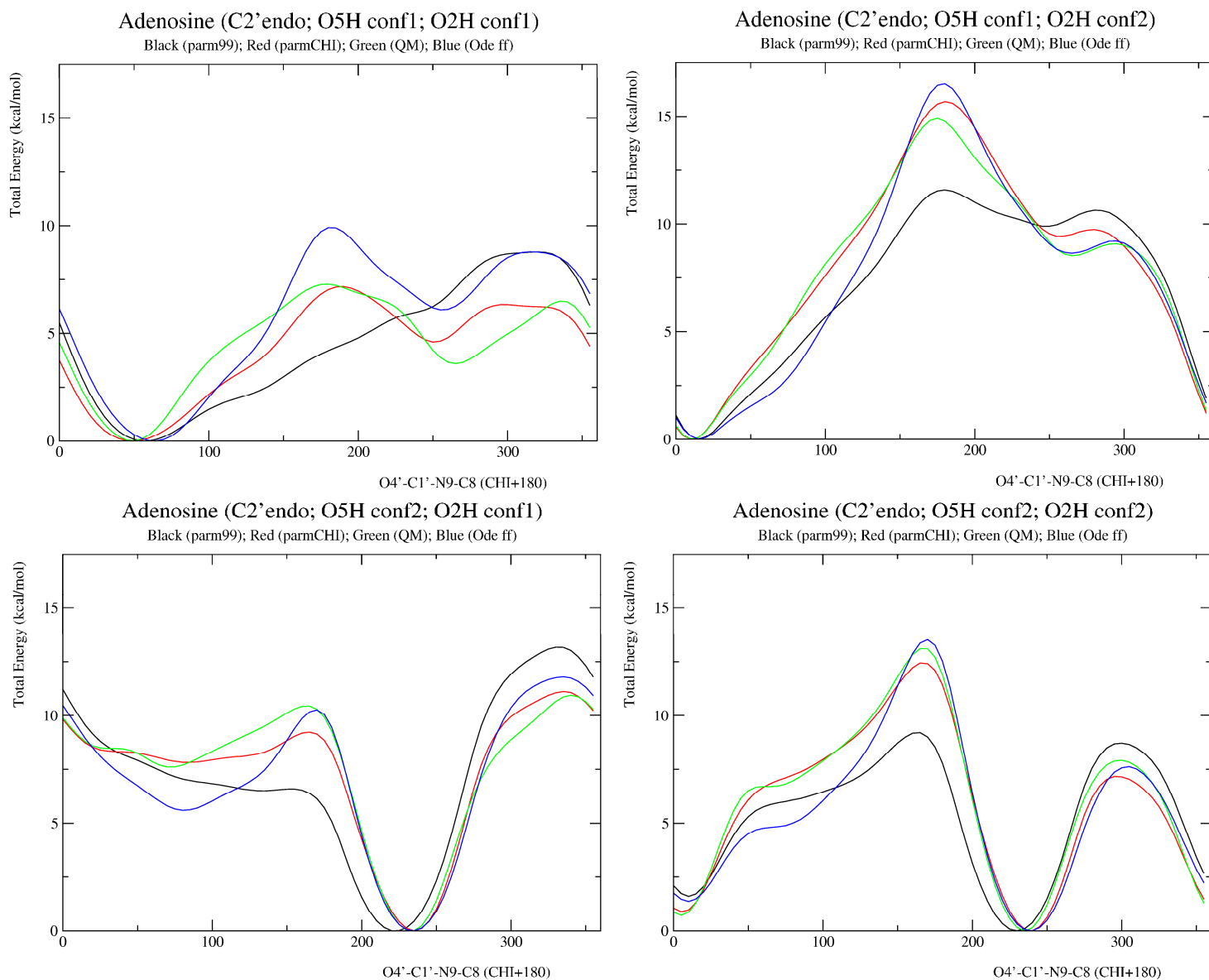


Figure S2. Testing how well AMBER99, AMBER99 χ , and Ode force fields mimic the quantum mechanical energy surface of adenosine when sugar pucker is C3'endo. Conformations used are defined in Table S6. [parm99=AMBER99; parmCHI = AMBER99 χ]

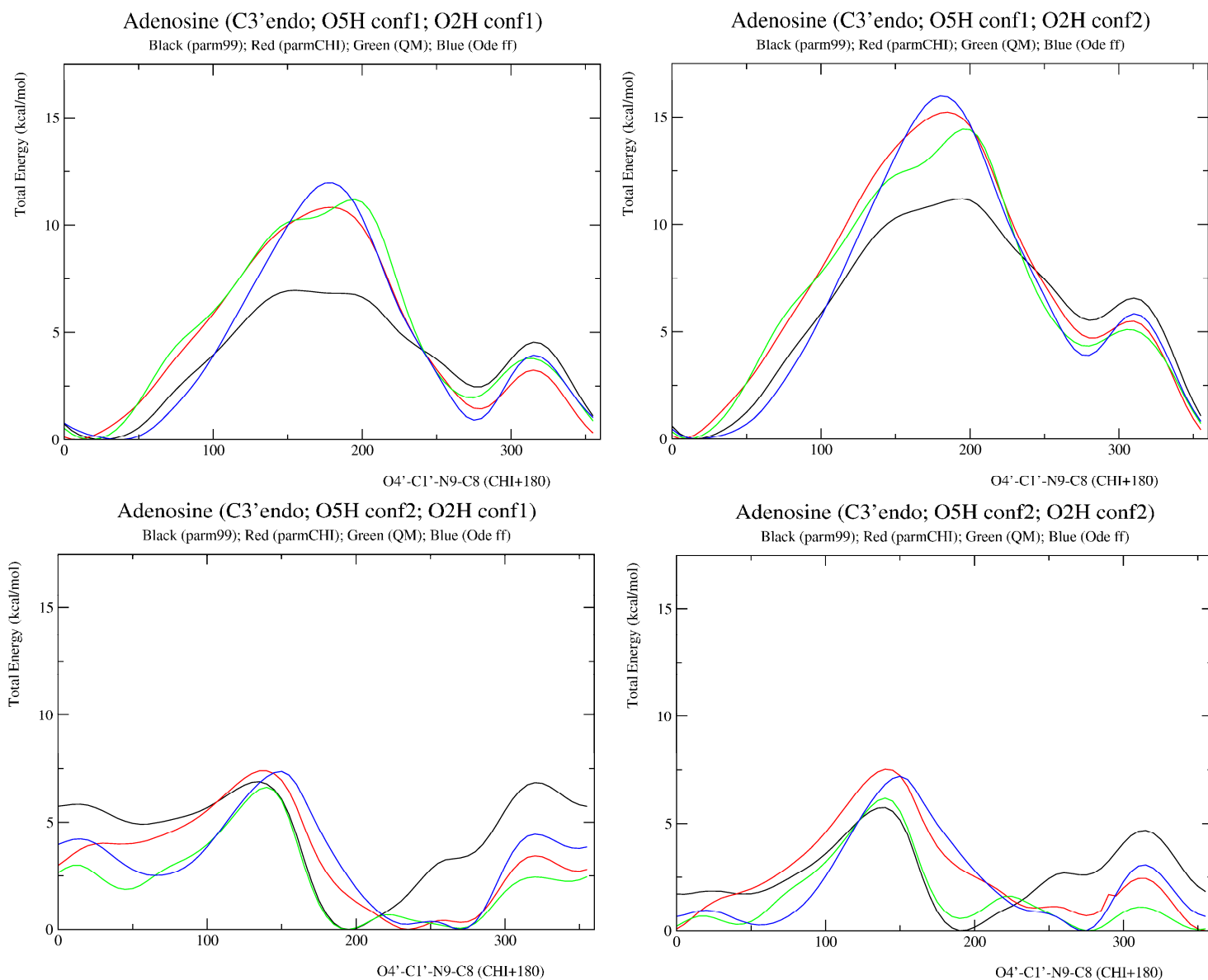


Figure S3. Testing how well AMBER99, AMBER99 χ , and Ode force fields mimic the quantum mechanical energy surface of adenosine when sugar pucker is O4'endo. Conformations used are defined in Table S6. [parm99=AMBER99; parmCHI = AMBER99 χ]

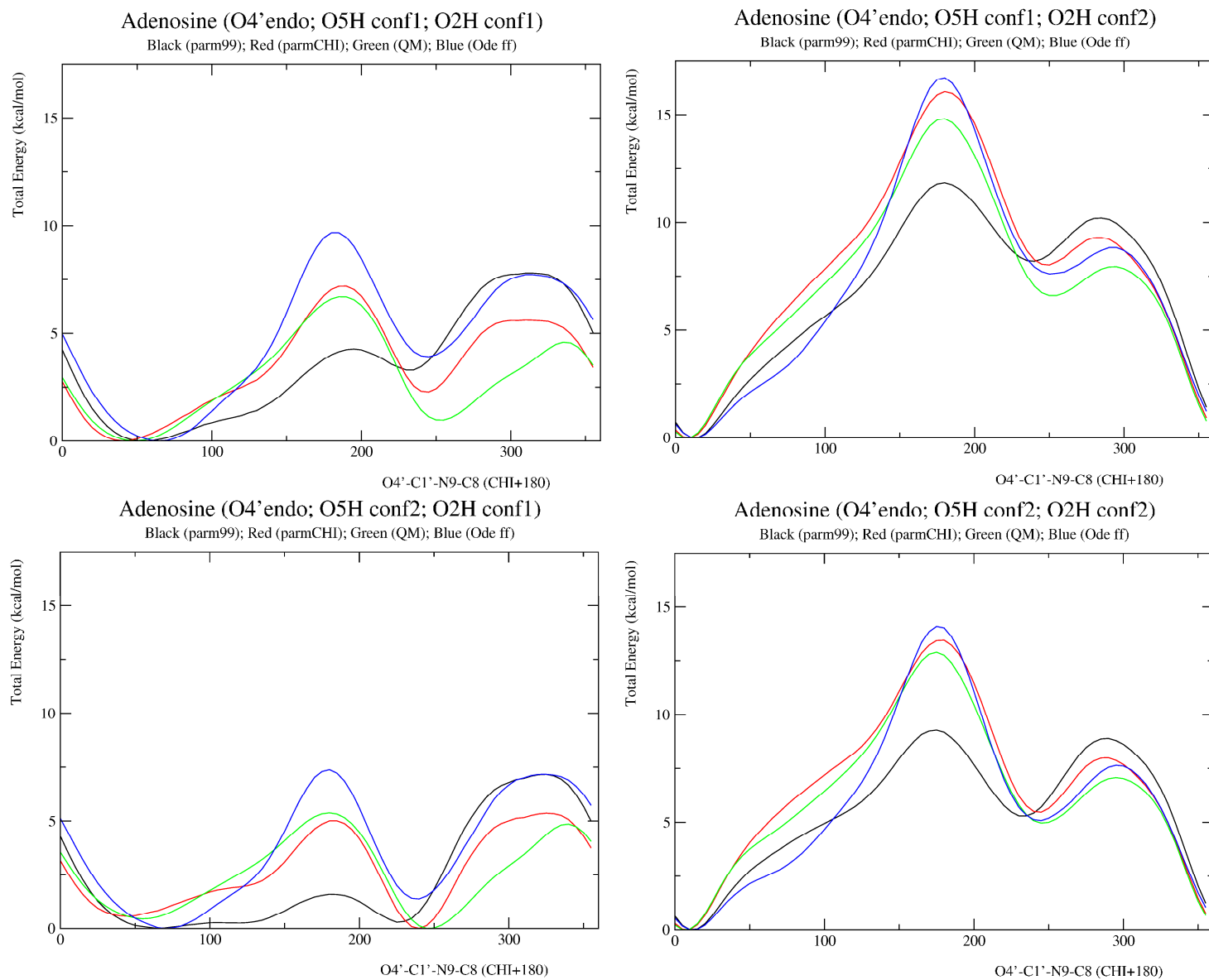


Figure S4. Testing how well AMBER99, AMBER99 χ , and Ode force fields mimic the quantum mechanical energy surface of guanosine when sugar pucker is C2'endo. Conformations used are defined in Table S6. [parm99=AMBER99; parmCHI = AMBER99 χ]

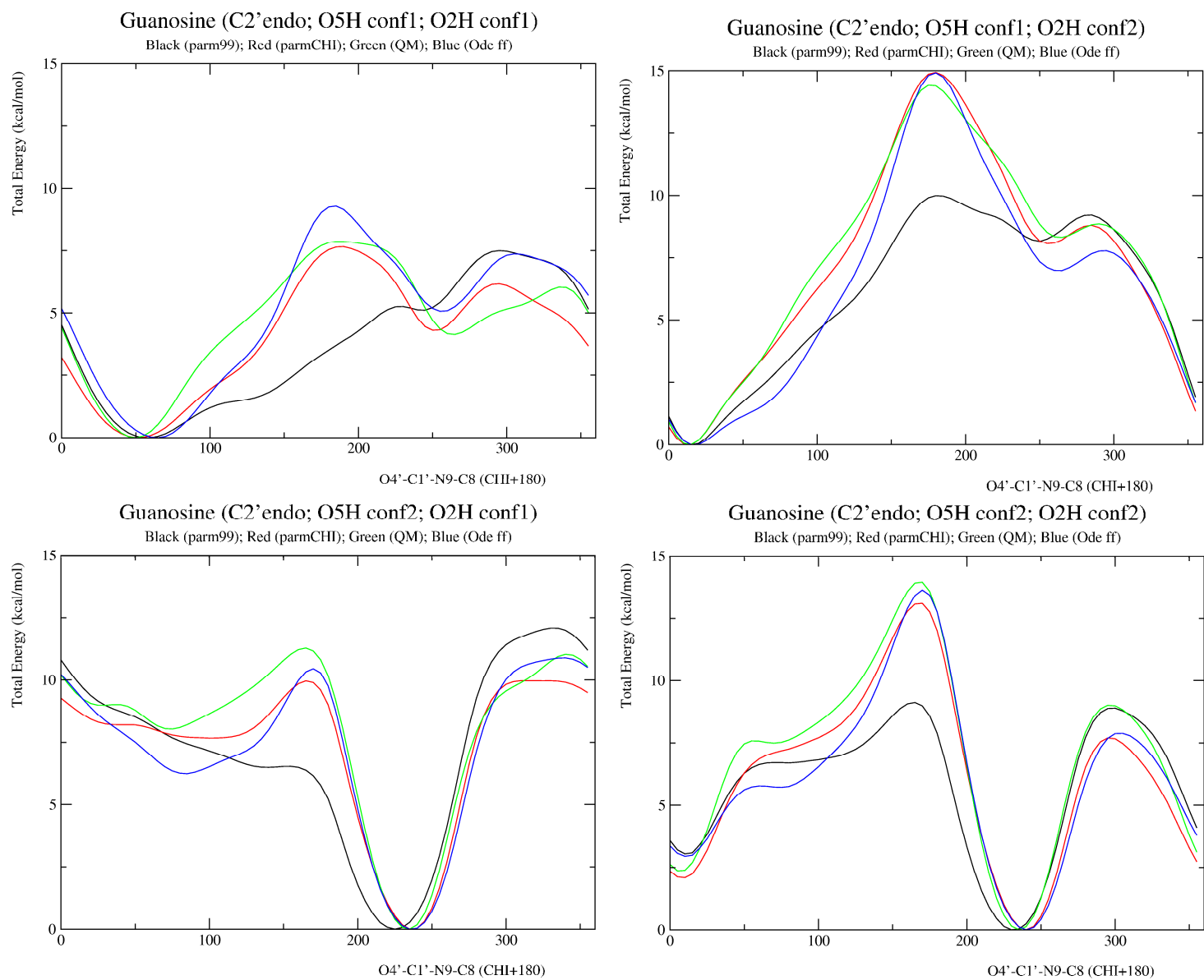


Figure S5. Testing how well AMBER99, AMBER99 χ , and Ode force fields mimic the quantum mechanical energy surface of guanosine when sugar pucker is C3'endo. Conformations used are defined in Table S6. [parm99=AMBER99; parmCHI = AMBER99 χ]

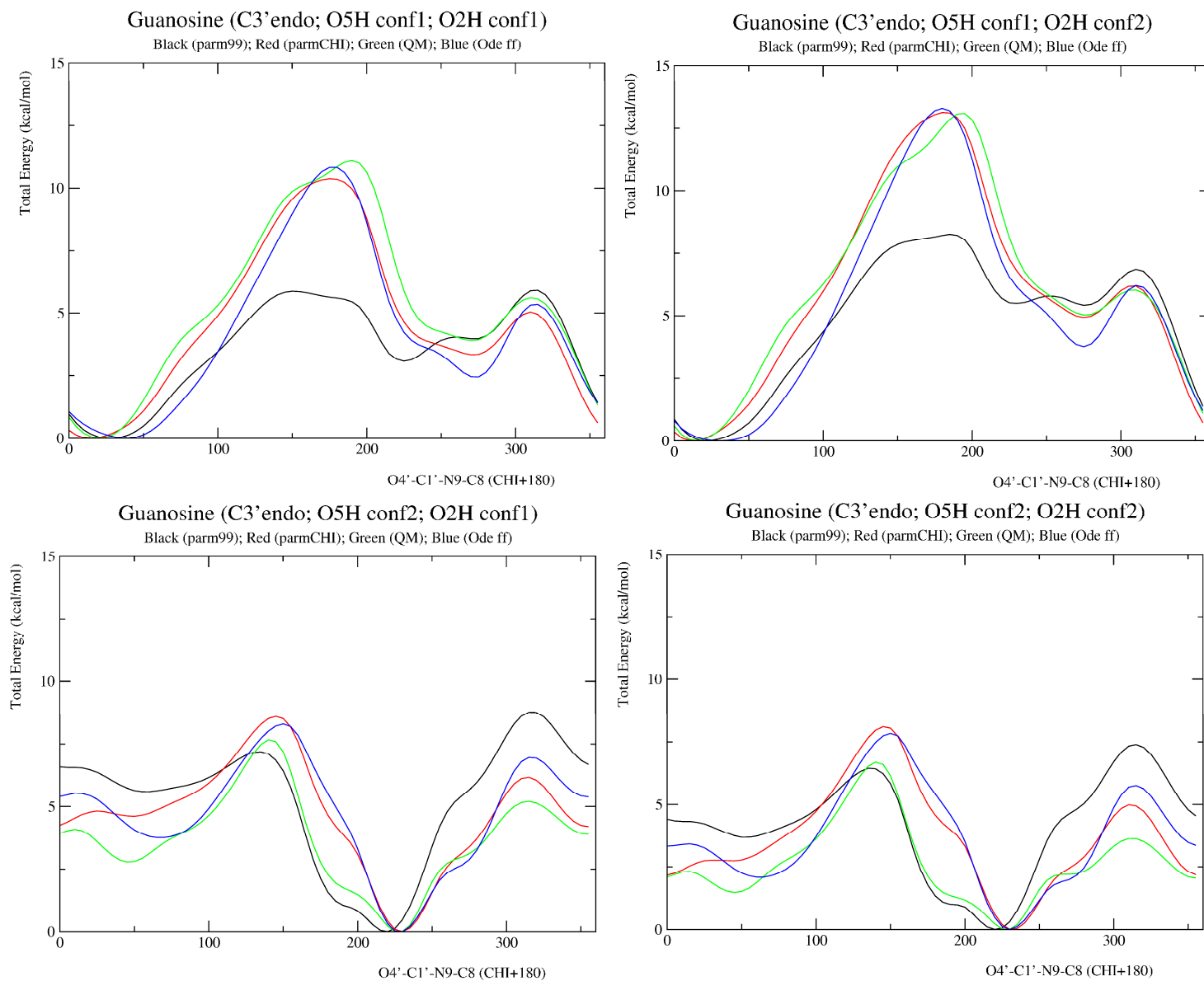


Figure S6. Testing how well AMBER99, AMBER99 χ , and Ode force fields mimic the quantum mechanical energy surface of guanosine when sugar pucker is O4'endo. Conformations used are defined in Table S6. [parm99=AMBER99; parmCHI = AMBER99 χ]

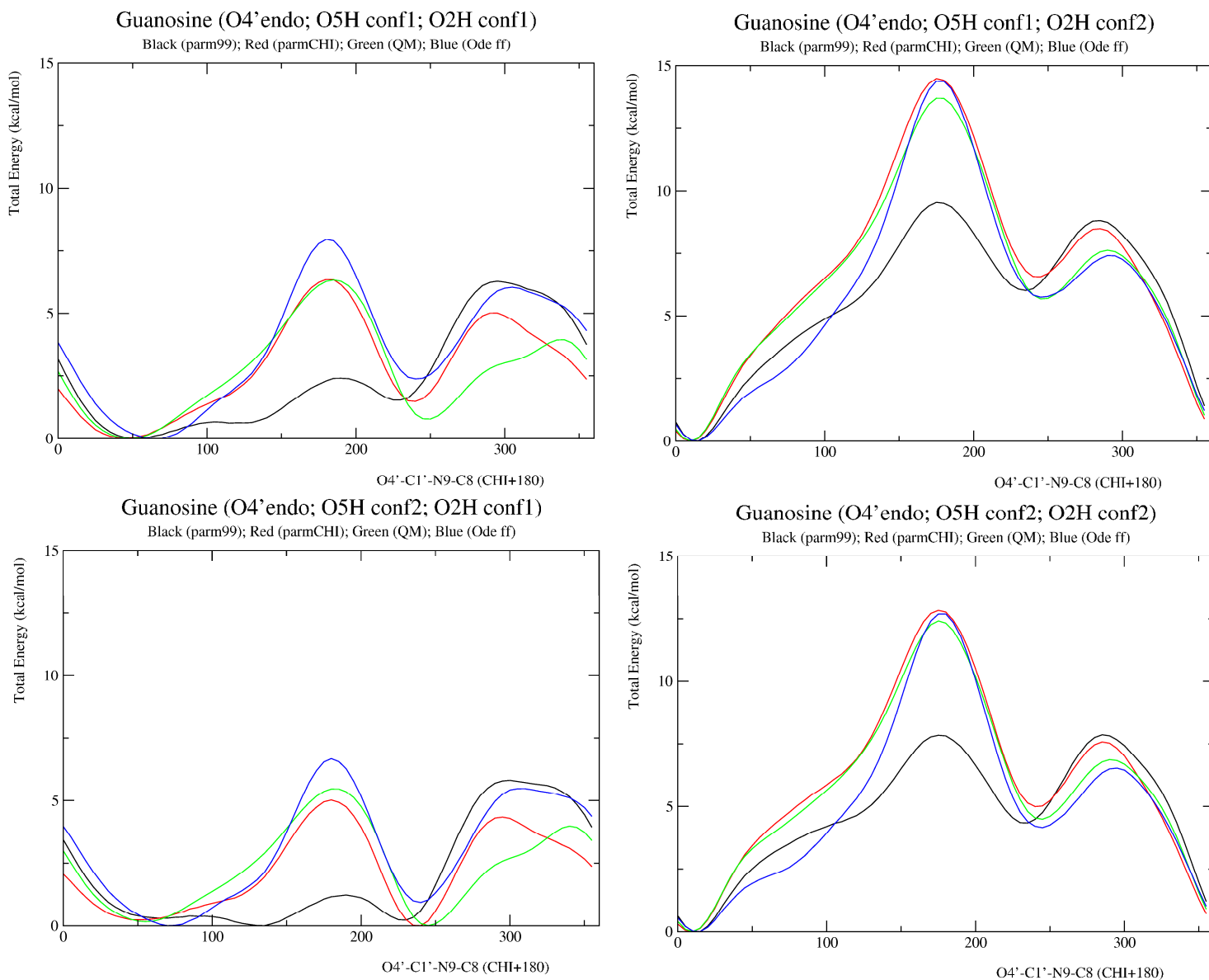


Figure S7. Testing how well AMBER99, AMBER99 χ , and Ode force fields mimic the quantum mechanical energy surface of cytidine when sugar pucker is C2'endo. Conformations used are defined in Table S6. [parm99=AMBER99; parmCHI = AMBER99 χ]

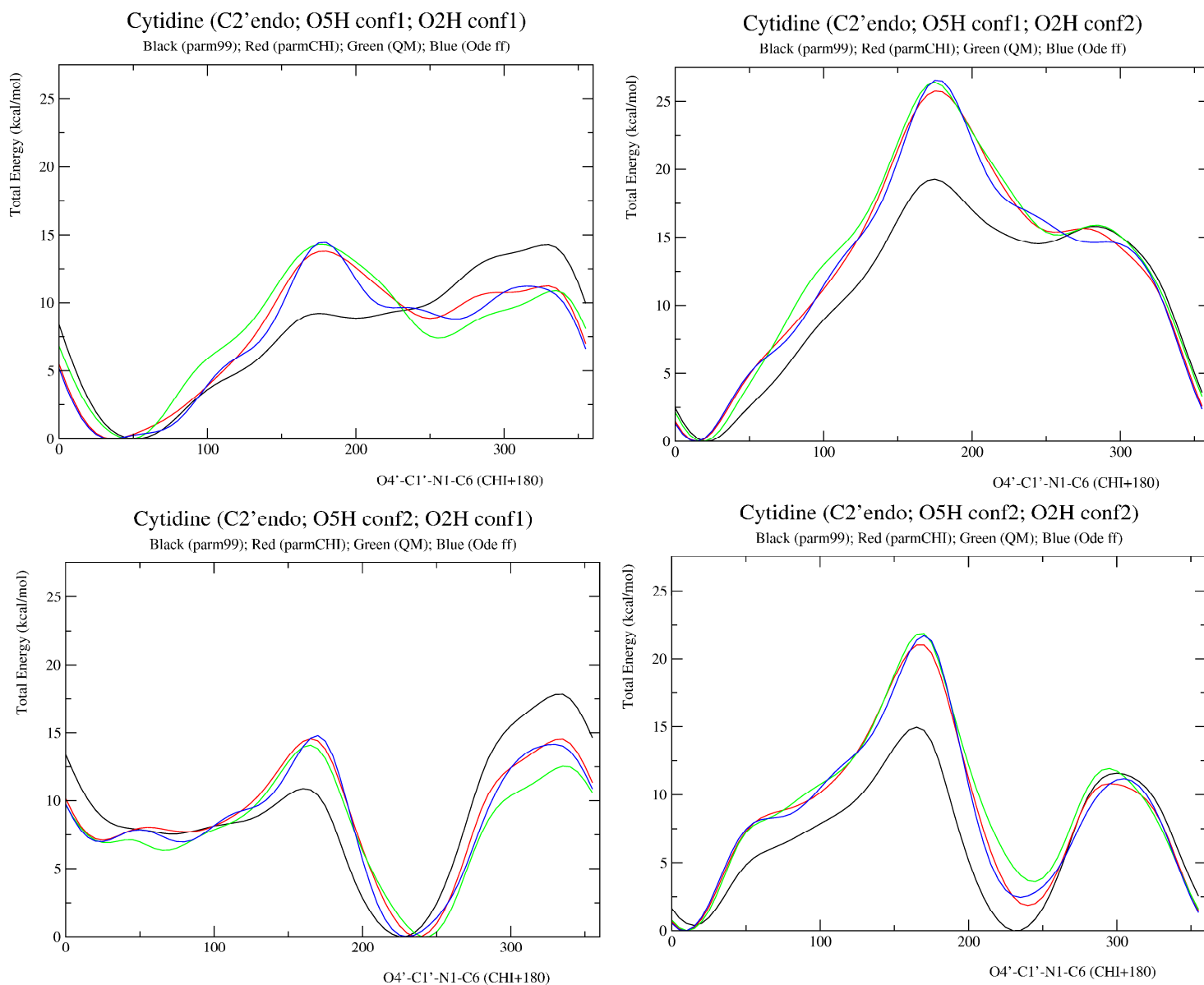


Figure S8. Testing how well AMBER99, AMBER99 χ , and Ode force fields mimic the quantum mechanical energy surface of cytidine when sugar pucker is C3'endo. Conformations used are defined in Table S6.
[parm99=AMBER99; parmCHI = AMBER99 χ]

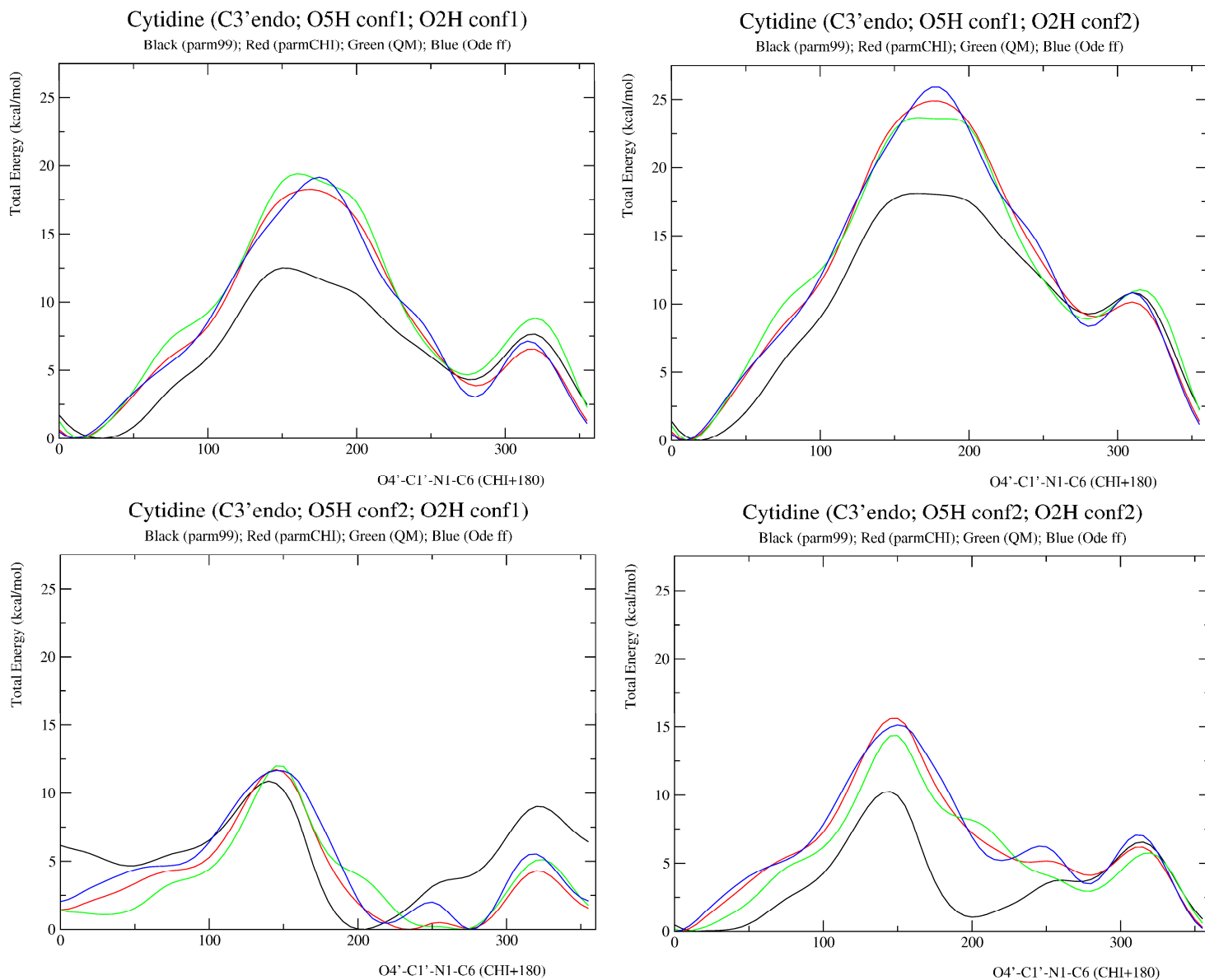


Figure S9. Testing how well AMBER99, AMBER99 χ , and Ode force fields mimic the quantum mechanical energy surface of cytidine when sugar pucker is O4'endo. Conformations used are defined in Table S6. [parm99=AMBER99; parmCHI = AMBER99 χ]

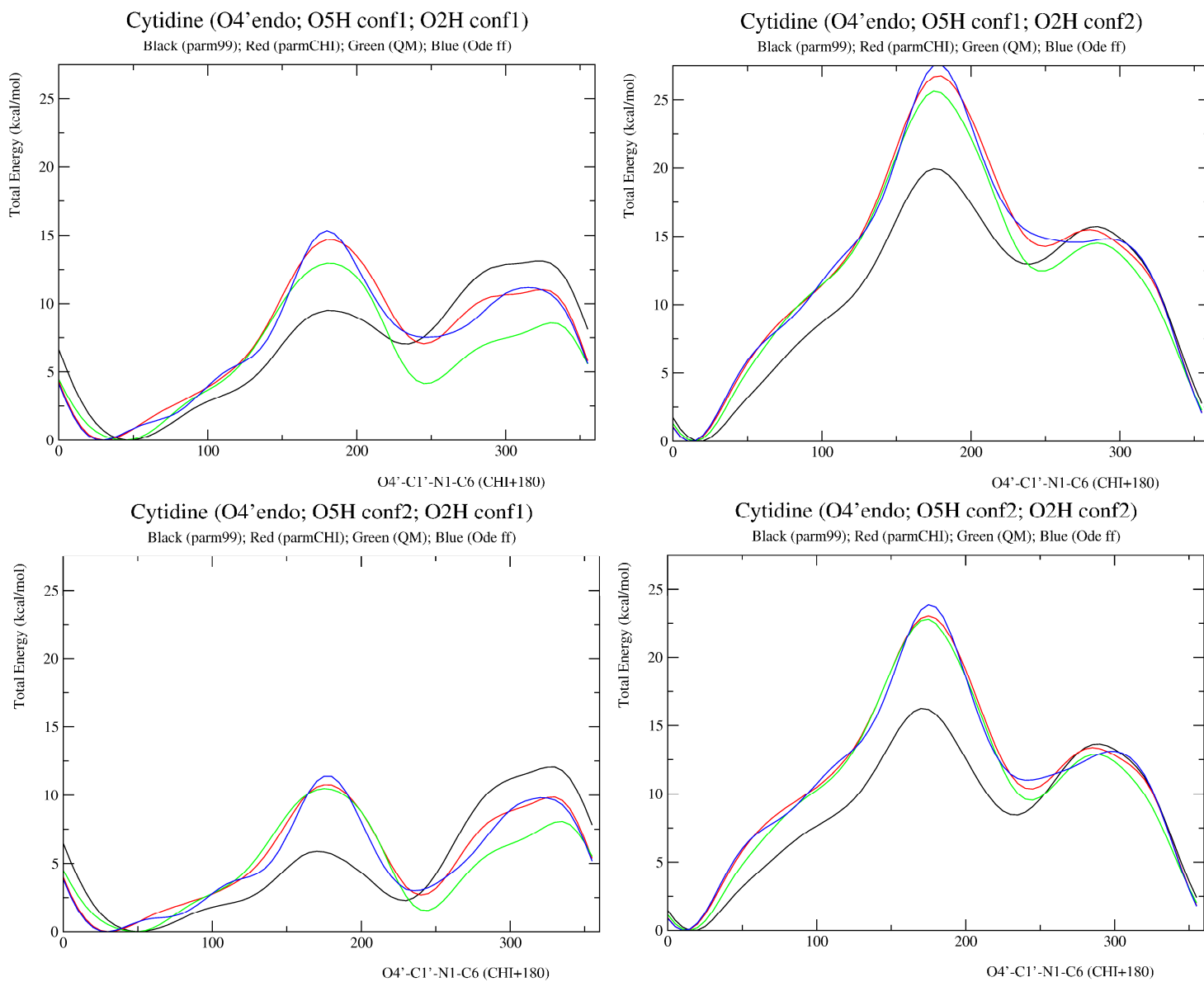


Figure S10. Testing how well AMBER99, AMBER99 χ , and Ode force fields mimic the quantum mechanical energy surface of uridine when sugar pucker is C2'endo. Conformations used are defined in Table S6. [parm99=AMBER99; parmCHI = AMBER99 χ]

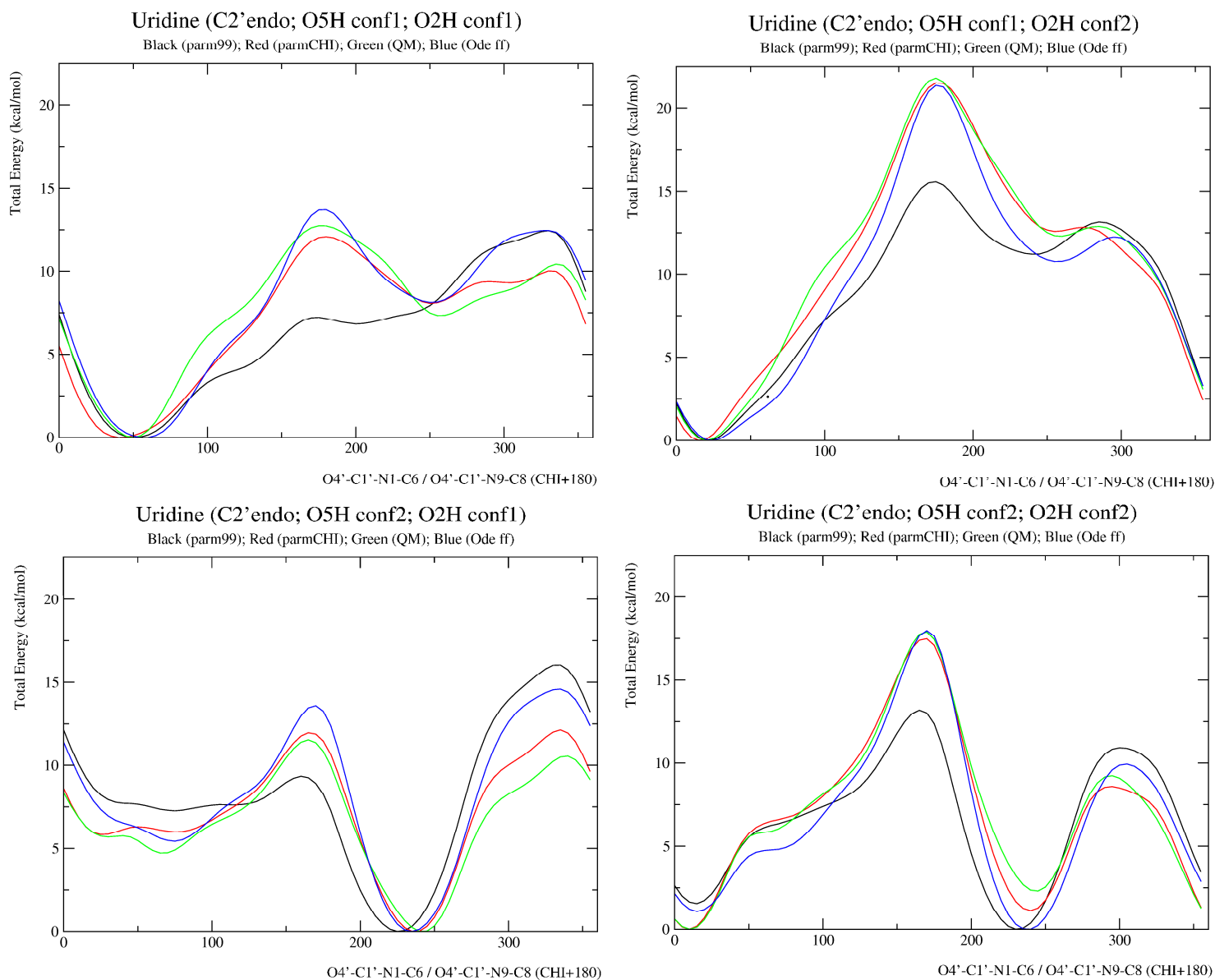


Figure S11. Testing how well AMBER99, AMBER99 χ , and Ode force fields mimic the quantum mechanical energy surface of uridine when sugar pucker is C3'endo. Conformations used are defined in Table S6. [parm99=AMBER99; parmCHI = AMBER99 χ]

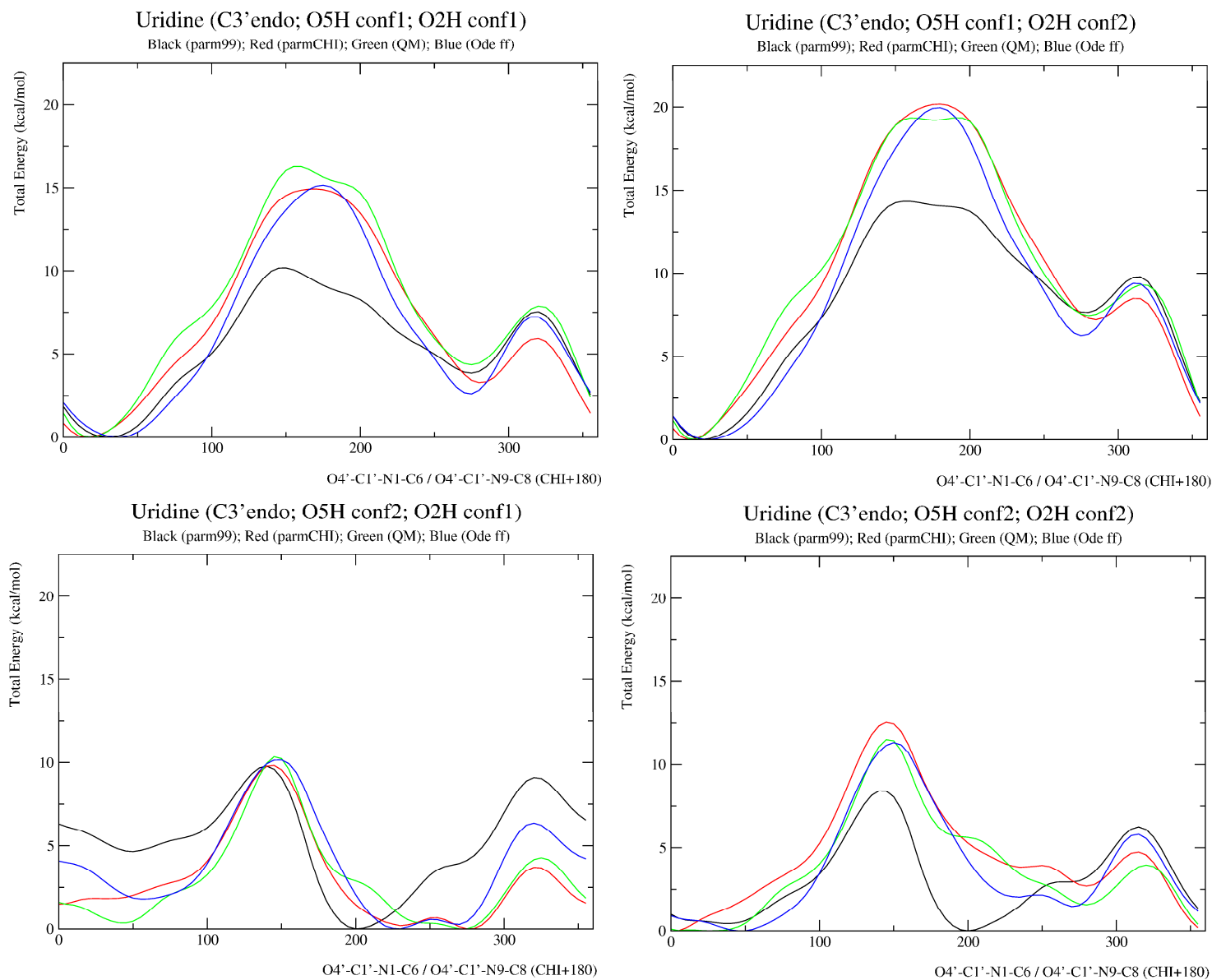


Figure S12. Testing how well AMBER99, AMBER99 χ , and Ode force fields mimic the quantum mechanical energy surface of uridine when sugar pucker is O4'endo. Conformations used are defined in Table S6. [parm99=AMBER99; parmCHI = AMBER99 χ]

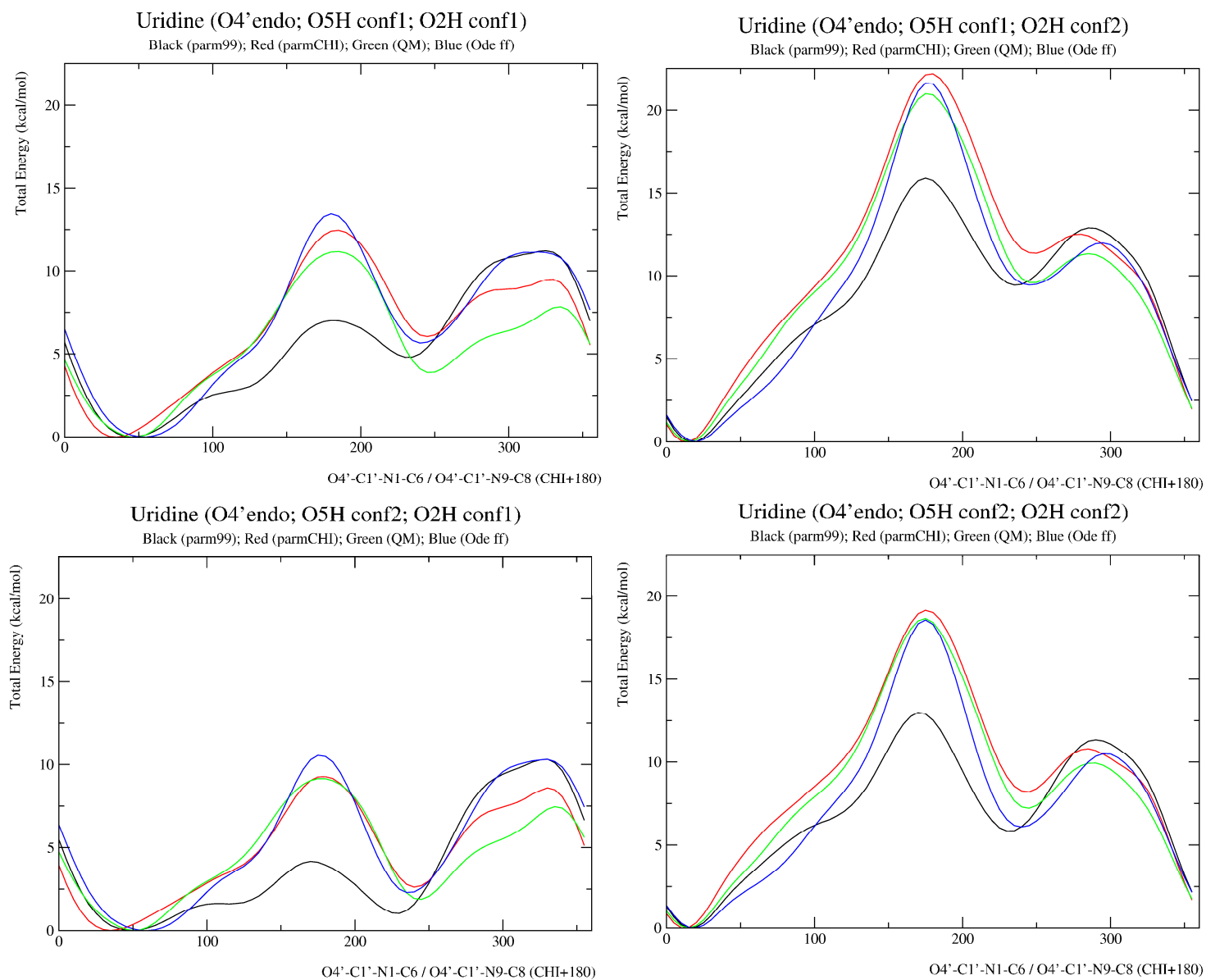


Figure S13. Intensity vs. mixing time plot of H5, H2', and H1' protons in transient NOE NMR experiment for 5 mM sample of cytidine at 10 °C. Mixing time region 0.2-0.4 s corresponds to the linear region.

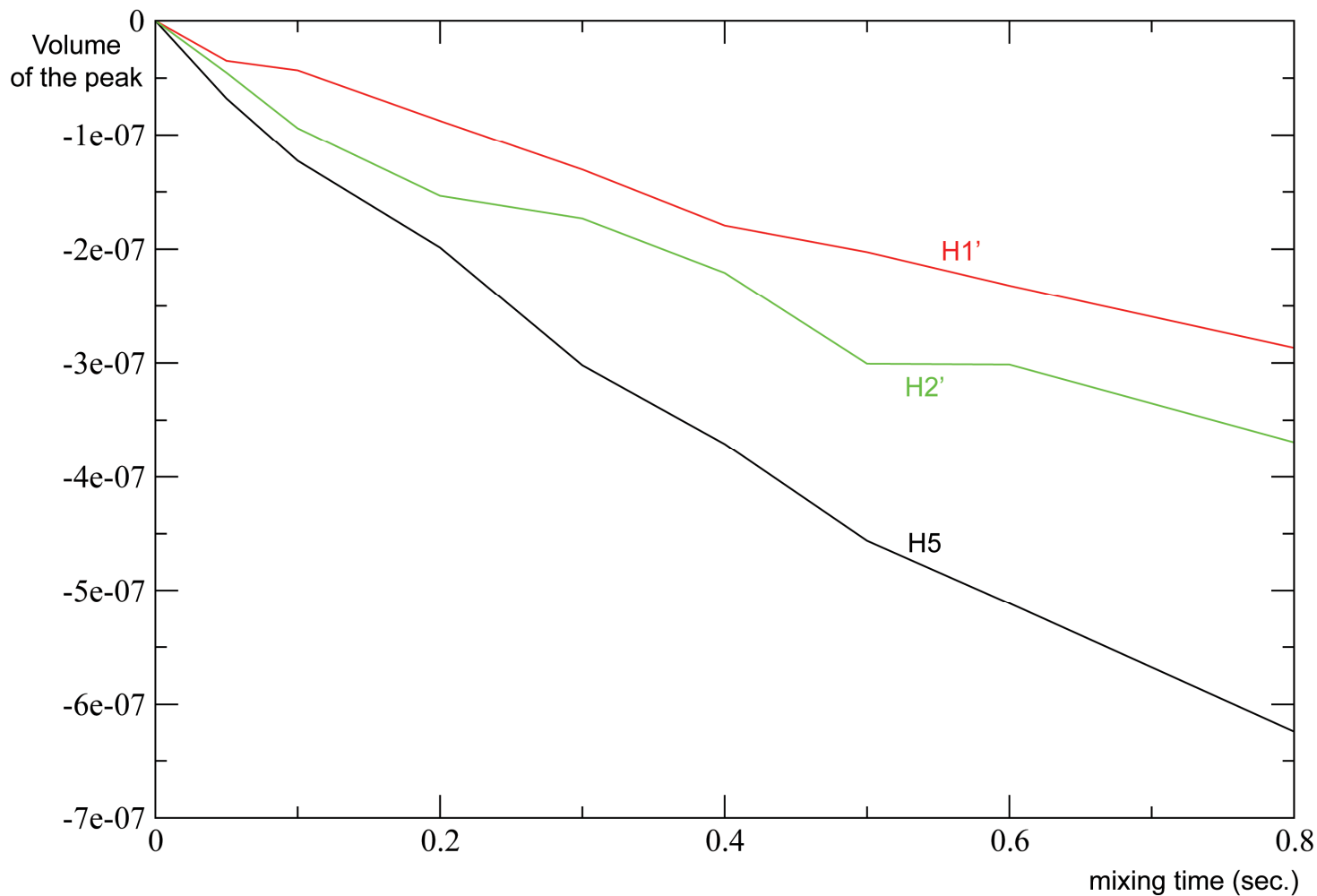


Figure S14. Intensity vs. mixing time plot of H5, H2', and H1' protons in transient NOE NMR experiment for 5 mM sample of uridine at 10 °C. Mixing time region 0.2-0.4 s corresponds to the linear region.

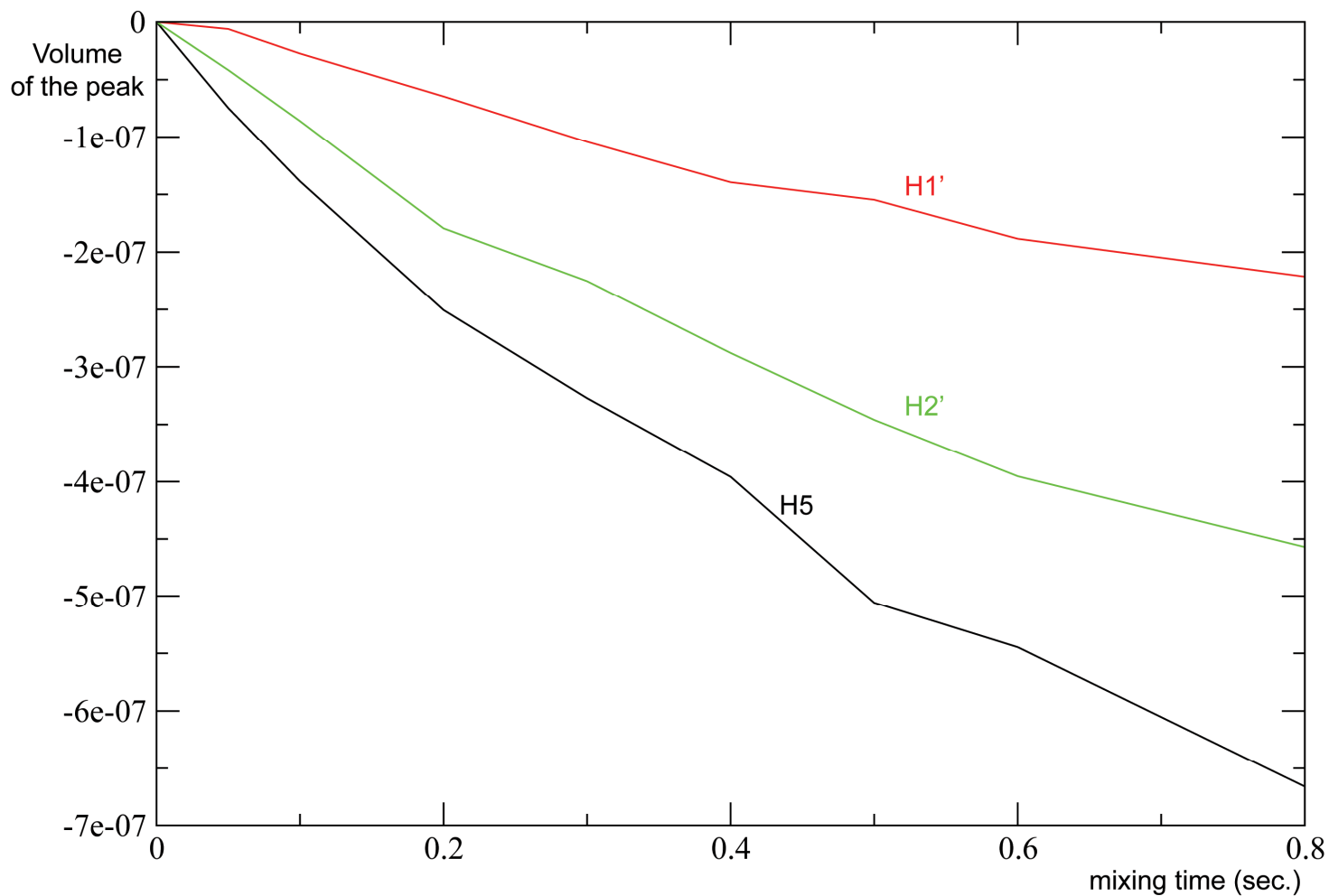


Figure S15. RMSD (\AA) vs. time (ns) plots of combined MD simulations of (a) adenosine with AMBER99, (b) adenosine with AMBER99 χ , (c) guanosine with AMBER99, and (d) guanosine with AMBER99 χ . Each 30 ns corresponds to individual MD simulations. At each 10 ps time, snapshots in the trajectory files are extracted and RMSD fit to a C3'endo anti type base orientation. RMSD around 2-2.5 \AA corresponds to a syn type base orientation while RMSD around 0.5-1 \AA corresponds to an anti type base orientation.

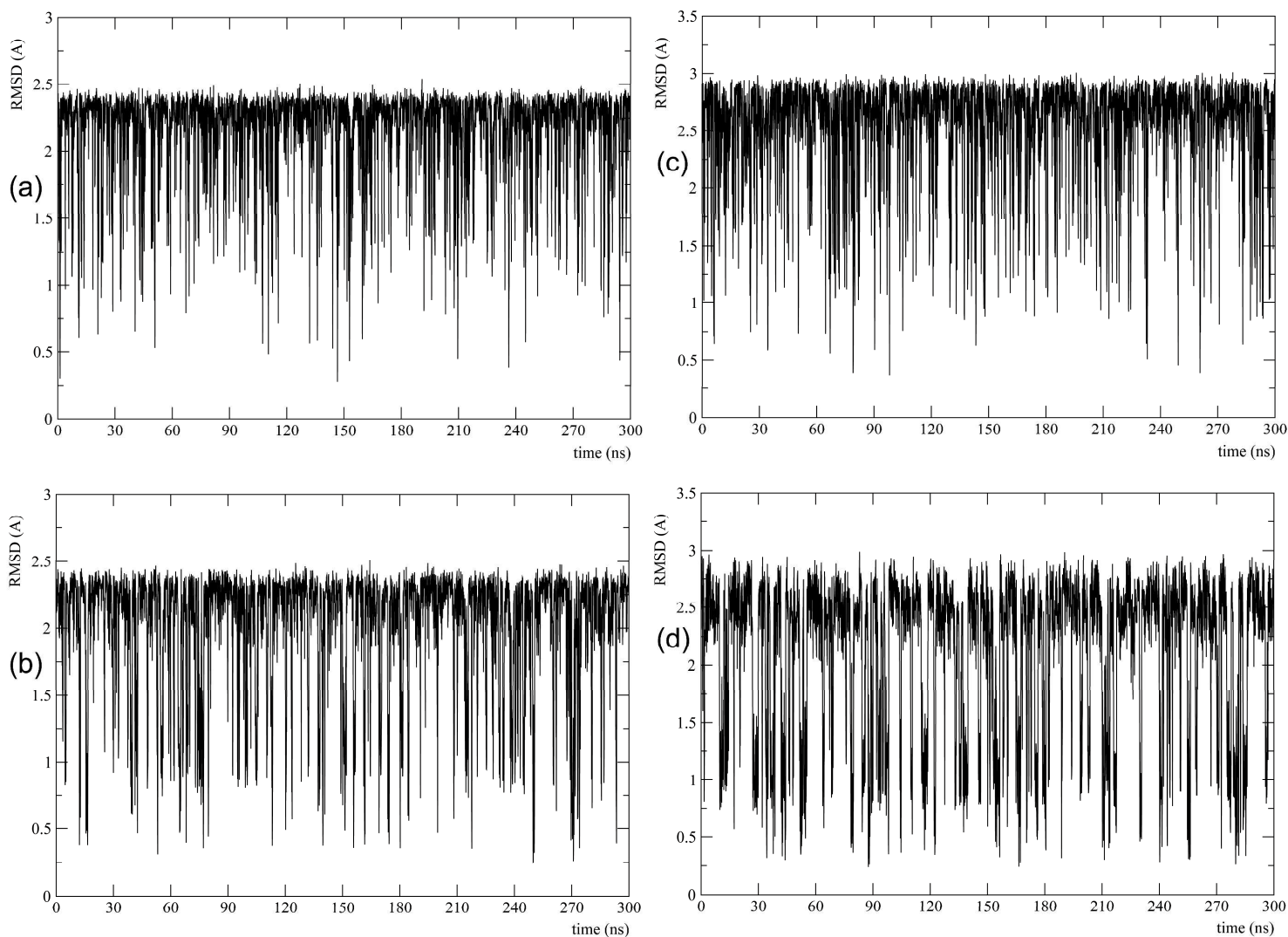


Figure S16. RMSD (\AA) vs. time (ns) plots of combined MD simulations of (a) cytidine with AMBER99, (b) cytidine with AMBER99 χ , (c) uridine with AMBER99, and (d) uridine with AMBER99 χ . Except for b, each 30 ns corresponds to individual MD simulations. In b, each 120 ns corresponds to individual MD simulations. At each 10 ps time, snapshots in the trajectory files are extracted and RMSD fit to a C3'endo anti type base orientation. RMSD around 2.0 \AA corresponds to a syn type base orientation while RMSD around 1.0 \AA corresponds to an anti type base orientation. Except for b, the simulations in the first 150 ns (180 ns for b) were started from a syn conformation, and the following simulations were started in an anti conformation. Note that syn type base orientation is favored by AMBER99 ff for pyrimidines.

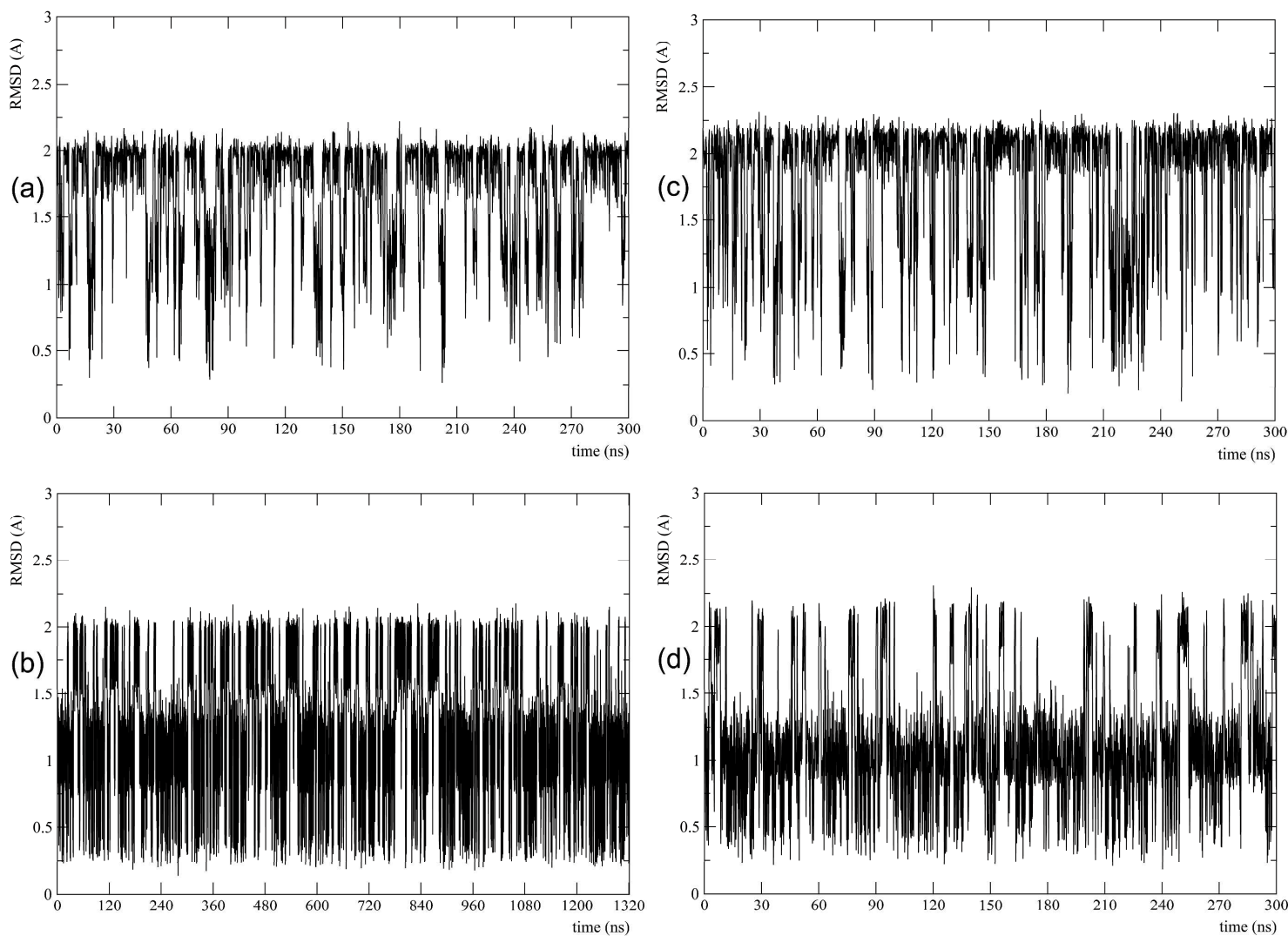


Figure S17. Population distribution (frequency vs. χ torsion) of MD simulations of (a) cytidine with AMBER99, (b) cytidine with AMBER99 χ , (c) uridine with AMBER99, and (d) uridine with AMBER99 χ . Black curves represent the population distribution of the combined MD simulations when the starting structure is in an anti type base orientation while red curves represent the population distribution of the combined MD simulations when the starting structure is in a syn type base orientation. (b) was scaled down to be compatible with the other plots because of the simulation time. These plots show that a converged population distribution is reached.

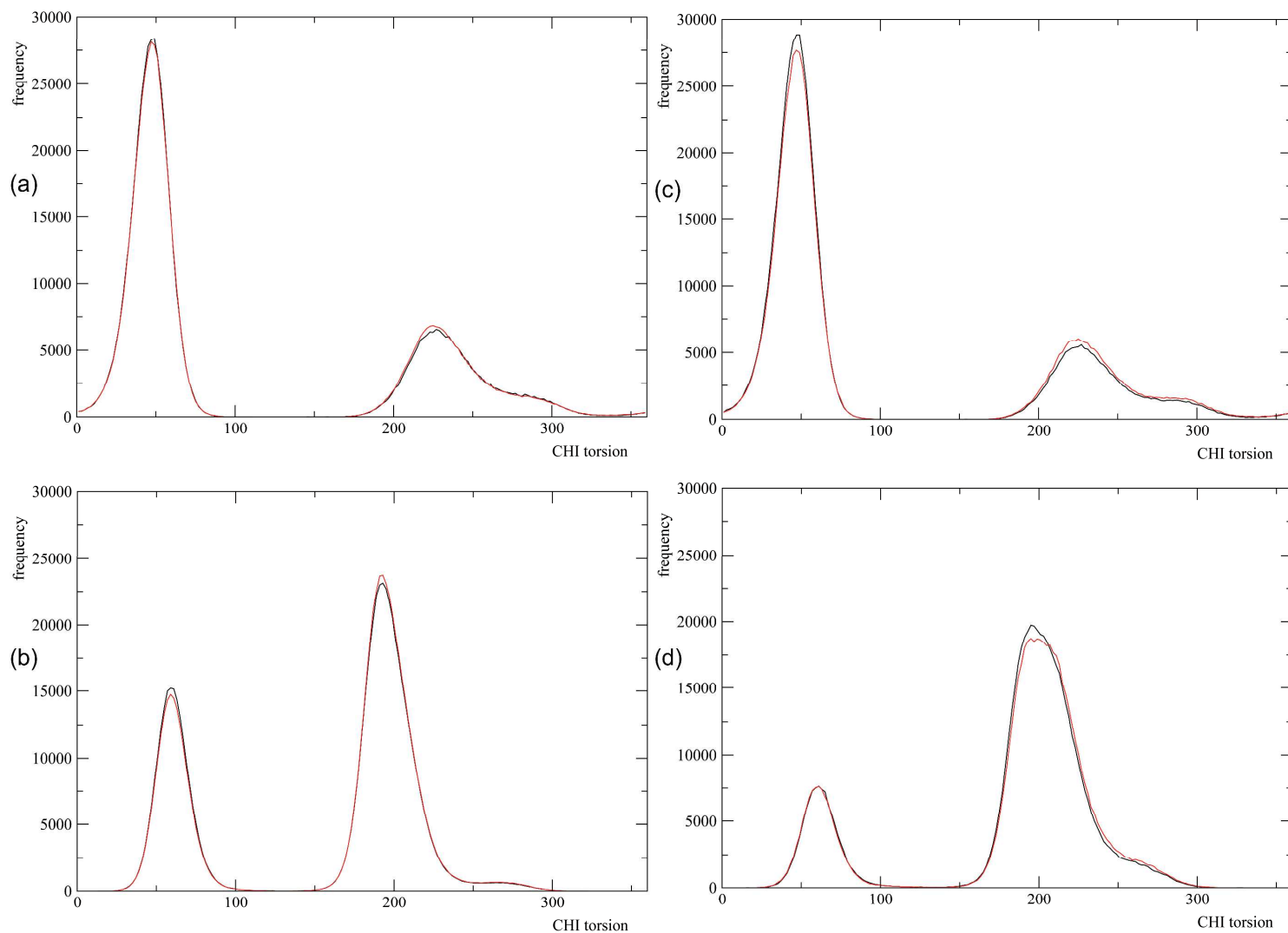
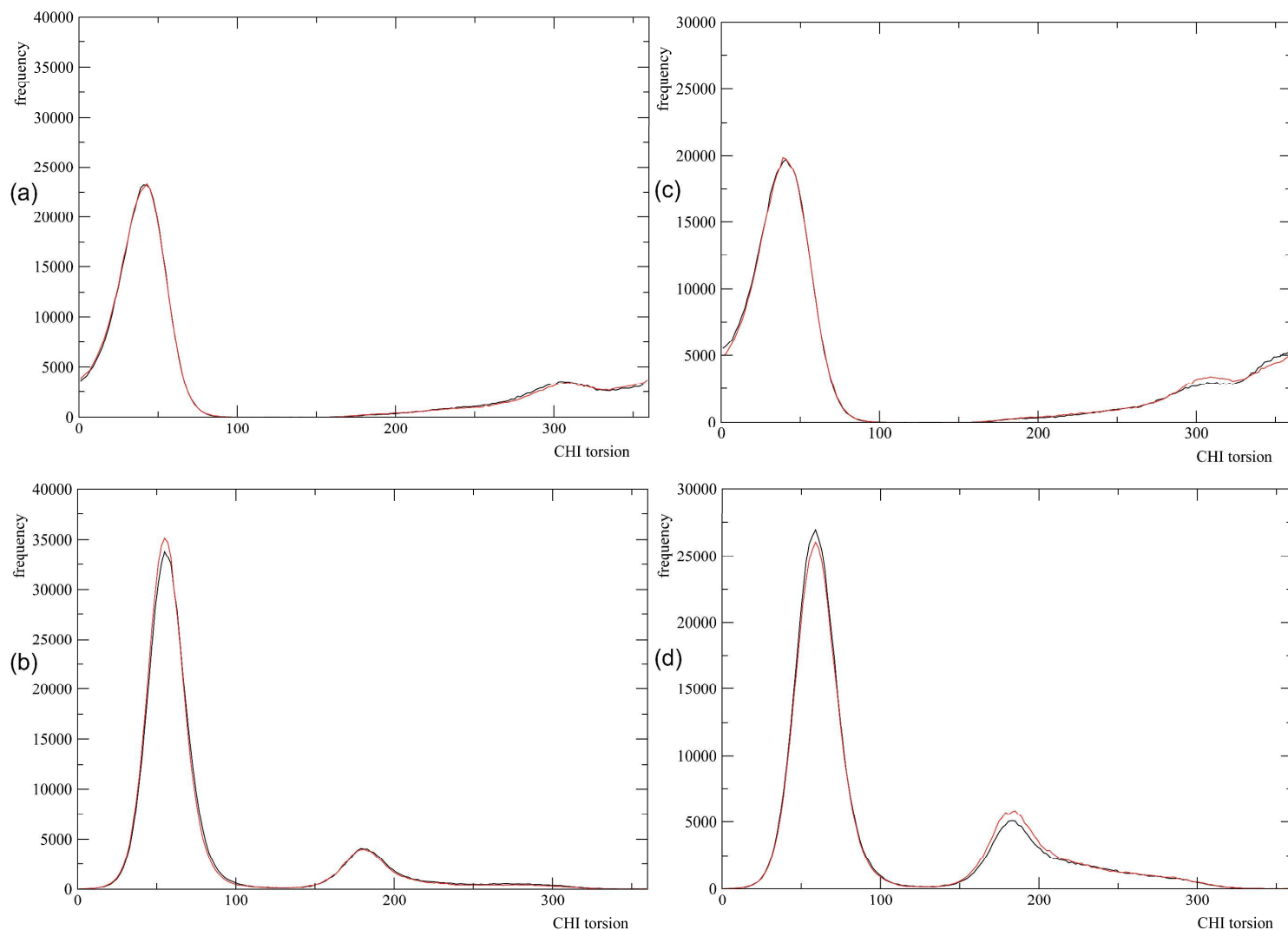


Figure S18. Population distribution (frequency vs. χ torsion) of MD simulations of (a) adenosine with AMBER99, (b) adenosine with AMBER99 χ , (c) guanosine with AMBER99, and (d) guanosine with AMBER99 χ . Black curves represent the population distribution of the combined MD simulations when the starting structure is in an anti type base orientation while red curves represent the population distribution of the combined MD simulations when the starting structure is in a syn type base orientation. These plots show that a converged population distribution is reached.



References

1. Chang, Y. C.; Herath, J.; Wang, T. H. H.; Chow, C. S. Synthesis and solution conformation studies of 3-substituted uridine and pseudouridine derivatives. *Bioorg. Med. Chem.* **2008**, *16*, 2676.